HUMAN PLURIPOTENT STEM CELL-DERIVED MESOTHELIUM FUNCTIONS IN REGENERATIVE MEDICINE AS A MULTIPOTENT VASCULAR PROGENITOR

by

THOMAS ANTHONY COLUNGA

(Under the Direction of Stephen Dalton)

ABSTRACT

The human body contains two major coelomic cavities, thoracic and abdominal, that are lined with an epithelial cell called mesothelium. Mesothelium also forms the outer layer of internal organs within these cavities and an additional protective pouch surrounding the heart called the pericardium. Mesothelium contributes to the development of the coelomic organs including the vasculature by acting as a multipotent vascular progenitor. During development and upon reactivation after injury, the mesothelium of the outer layer of organs loses its polarity and migrates to the underlying tissue in a process called epithelial-to-mesenchymal transition (EMT). After undergoing EMT, mesothelium can differentiate to vascular lineages required for the growth of new blood vessels that play an important role in organ repair and regeneration processes. For these reasons, mesothelium constitutes a resident vascular progenitor cell type found in all coelomic organs including the heart, lung, liver and gut and may have utility in regenerative medicine. Utilizing human pluripotent stem cells (hPSCs), we have developed an *in vitro*-derived mesothelial cell (MesoT) that can give rise to all the required vascular lineages. When using MesoT as a cellular therapeutic for a

mechanically injured neonatal mouse model we uncovered its ability to incorporate into newly formed blood vessels. MesoT cells were also used to reseed the vascular network of a decellularized biological scaffold. Subsequent *in vivo* implantation of the newly vascularized graft displayed patency, did not thrombose and was able to perfuse blood down to the capillary bed which confirmed its utility in tissue engineering and possible corrective surgery. This work constitutes one of the first reports of a true vascular progenitor that can give rise to all required cell types of the vasculature and highlights the utility of MesoT cells in regenerative medicine.

INDEX WORDS: mesothelium, human pluripotent stem cells, vascular progenitor cells, cellular therapy, tissue engineering, regenerative medicine, blood vessel

HUMAN PLURIPOTENT STEM CELL-DERIVED MESOTHELIUM FUNCTIONS IN REGENERATIVE MEDICINE AS A MULTIPOTENT VASCULAR PROGENITOR

by

THOMAS ANTHONY COLUNGA

BS, University of Houston-Downtown, 2013

A Dissertation Submitted to the Graduate Faculty of The University of Georgia in Partial Fulfillment of the Requirements for the Degree

DOCTOR OF PHILOSOPHY

ATHENS, GEORGIA

2018

HUMAN PLURIPOTENT STEM CELL-DERIVED MESOTHELIUM FUNCTIONS IN REGENERATIVE MEDICINE AS A MULTIPOTENT VASCULAR PROGENITOR

by

THOMAS ANTHONY COLUNGA

Major Professor: Stephen Dalton
Committee: Robert Haltiwanger
Lianchun Wang
Amar Singh

Electronic Version Approved:

Suzanne Barbour
Dean of the Graduate School
The University of Georgia
May 2018

DEDICATION

This work is dedicated to my parents, siblings, nieces and nephews. You have never stopped believing in me and were always there when I needed you the most. You helped me through all the rough times and celebrated with me during the good times. This degree would not have been possible without your love and support. I don't think there is anything I could do to repay each of you but I will spend the rest of my life trying. This is proof that our family can overcome anything and succeed. I love you!

I would also like to dedicate this to the memory of family and friends that are gone but not forgotten. You are truly missed.

ACKNOWLEDGEMENTS

There are a few individuals I need to acknowledge that helped me get to this point in my life. I would like to start by thanking God for helping me see this vision through to the end and allowing me to accomplish so much. I also need to acknowledge my extended family who gave me so much support and encouragement and truly believed that I was capable of obtaining my Ph.D.

I also need to acknowledge and thank Dr. Stephen Dalton for the support and guidance he has given me throughout my graduate education. His mentorship coupled with those of my advisory committee have been crucial in my development as a scientist. I would also like to acknowledge the collaborators and previous lab members who helped with this project.

Lastly, I would like to acknowledge the Natural Sciences department at the University of Houston-Downtown for providing me with a great educational experience and rigorous degree. Dr. Lisa Morano was particularly helpful in guiding and encouraging me to pursue research and graduate education. She was vital in helping me land my first research opportunity and I have never looked back since. Dr. Phil Lyons also played a big role by trusting me to conduct research in his lab and I will always be grateful for that experience. Attending the University of Houston-Downtown forever changed my life and will be considered one of the best investments I ever made.

TABLE OF CONTENTS

Page

LIST OF TABLES

Page

LIST OF FIGURES

Page

CHAPTER 1

INTRODUCTION AND LITERATURE REVIEW

Regenerative Medicine

Basic science and biomedical research have led to tremendous fundamental discoveries that laid the foundation for the field of regenerative medicine. This field blends the research lab and clinical settings and actually encompasses two subsets; cellular therapy and tissue engineering. One of the goals of regenerative medicine is to restore the function and structure of organs and tissues that have been damaged due to disease or injury. Another more ambitious goal is to generate fully functional organs in the lab from natural and/or synthetic components that can eventually help meet the increasing demand for organ transplantation. Patients needing heart, liver or kidney transplants typically wait years for available organs while their quality of life and health steadily decline. From 2011-2012, less than 40% of patients needing a kidney transplant received the organ within 5 years and less than 10% of the global organ transplant need was met [1]. This constitutes a major world health crisis that is being exacerbated by rapidly increasing incidences of diabetes and cardiovascular disease [2]. Cellular therapy and tissue engineering are attempting to tackle these issues by utilizing human pluripotent stem cells (hPSCs) in a clinical setting.

The main distinguishing factor between cellular therapy and tissue engineering is the latter's use of a scaffold on which to build. Cellular therapy aims to replace cells of

failing, diseased or injured organs and tissues by transplanting equivalent or progenitor cells at or near the site of interest [3, 4]. One important factor that cellular therapy must contend with is the route of delivery. Evidence from recent analyses have shown that this greatly influences therapeutic benefit [5, 6]. Tissue engineered scaffolds typically do not have to contend with this problem since they must be directly applied and anastomosed or grafted to the organ or tissue of interest. Scaffolds can be composed of natural or synthetic materials to create a mold resembling the organ or tissue of interest onto which cells can be seeded [7, 8]. One extremely important component of all tissue engineered scaffolds and organs is the vasculature. In order to properly generate this component, regenerative medicine has turned to the use of primary isolated and hPSC-derived vascular progenitor cells which have the capacity to differentiate into required cell types such as endothelium, smooth muscle cells and pericytes. Mesothelium is one such cell that has the capacity to differentiate into required vascular lineages and has potentially broad use as it is resident in multiple organs [9-12].

What is Mesothelium?

The human body is segmented into coelomic cavities that house the internal organs. These cavities and the organs within them are lined with mesothelium (Figure 1.1) [12-14]. Developmentally, mesothelium is descendent from the lateral plate mesoderm and covers the organs with a single layer of epithelial cells [12, 15]. Mesothelium is characterized by tight cell junctions such as E-cadherin and ZO1 (Zona Occludens 1) and expression of transcription factors WT1 (Wilms tumor 1), TBX18 (T-Box protein 18) and TCF21 (Transcription factor 21) [16-18]. Some of the physiological

functions of mesothelium include acting as a physical barrier to prevent injury, inflammation response, secretion of growth factors and organ repair and regeneration [13, 19, 20]. Mesothelium also plays a role in deposition of extracellular matrix (ECM) which is extremely important for organ structural integrity and cell signaling. During organogenesis, the mesothelium contributes to multiple cell types including the vasculature [11, 21-25]. The most widely studied form of mesothelium is the epicardium (outer layer) of the heart. Epicardium forms after the proepicardial organ migrates to and engulfs the myocardial layer of the forming heart [26, 27]. The failure to generate a complete epicardial layer can lead to numerous defects such as incomplete development and compaction of the myocardium, missing coronary arteries and vessels and congenital heart defects [25, 26, 28-30]. Mesothelium typically exits the cell cycle and stops actively dividing after development to mainly function in a homeostatic role. However, physical injury or disease can trigger dynamic molecular changes reminiscent of embryonic mesothelium which has greater plasticity. This switch back to an early developmental program allows mesothelium to participate in the regeneration process of multiple organs by direct cellular contributions and release of cytokines and growth factors that stimulate cell survival and angiogenesis (Figure 1.2) [31].

Mesothelium is a Multipotent Vascular Progenitor

Embryonic and reactivated mesothelium contributes to the development and functional repair of organs by multiple mechanisms. The repair process is initiated by molecular changes that result in the loss of cell polarity via an epithelial-mesenchymal transition (EMT) [32, 33]. This change allows mesothelium to rearrange cytoskeletal

proteins and migrate to the underlying layers where they trans-differentiate into stromal or vascular cell types. Lineage tracing studies have shown that mesothelium gives rise to endothelium, smooth muscle cells and perivascular pericytes of blood vessels [10, 20, 29, 34]. This ability gives mesothelium clinical utility as a vascular progenitor cell that can be utilized in cellular therapy or tissue engineering. However, isolating primary mesothelial cells for these purposes is intrusive and yields low cell counts. To circumvent unnecessary surgical intrusions, researchers have developed mesothelial cells from hPSCs that can generate some of the in vivo vascular lineages [23, 35]. One of the main hurdles with current in vitro-derived mesothelium is downstream lineage restriction. To date, the field has yet to report a migratory or progenitor state of mesothelium which has the ability to fully recapitulate all the required vascular lineages and displays potential clinical utility in a regenerative medicine setting.

The work presented here attempts to address this need by developing a hPSC-derived mesothelium (MesoT) that displays migratory capacity, can differentiate into all vascular lineages (endothelium, smooth muscle cells, pericytes) and functions in regenerative medicine. This was done by first developing a directed differentiation protocol using defined media which allowed MesoT cells to progress through a splanchnic mesoderm state that mimics early development. Next, we characterized the epigenetic and transcriptional landscape of MesoT cells using a suite of sequencing methods which showed they clustered with native human and mouse mesothelium. MesoT epigenetic marks even revealed genes important for vascular specification to be in a primed state so we tested the ability of MesoT cells to generate functional endothelium and smooth muscle cells which are important for blood vessel generation. We then asked

if MesoT cells can function in cellular therapy or tissue engineering. This was done by transplanting cells using a neonatal mouse cardiac injury model to assess contribution to neo-vascularization. We followed up by using MesoT cells to revascularize a decellularized biological scaffold and implanting them into rats for 3 days. This work constitutes the first report of a true vascular progenitor cell that generated all the required vascular lineages, both in vitro and in vivo, and self-assemble into properly invested vessels. We also report the potential clinical utility of MesoT cells in cellular therapy and tissue engineering.

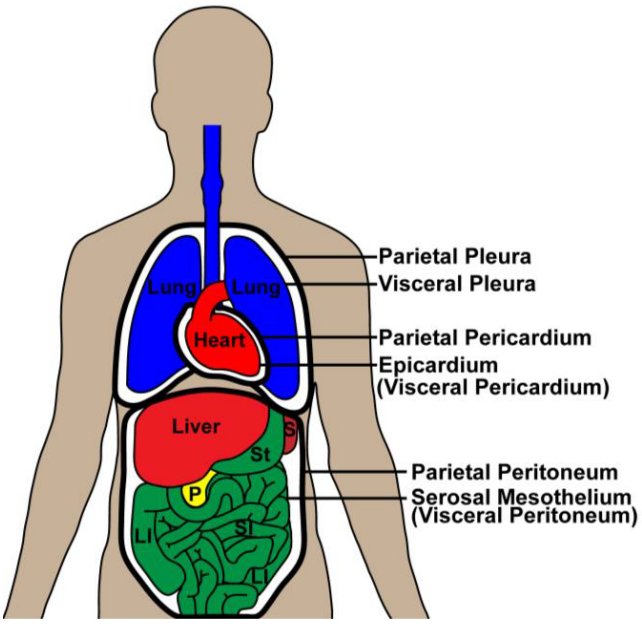

- Heart
- Liver
- Lung
- Gut
- Kidney
- Pancreas
- Spleen

Common molecular signature

$WT1^{+}$, $TBX18^{+}$, $ALDH1A2^{+}$, $TCF21^{+}$

Figure 1.1 Mesothelium lines the coelomic cavities and the organs within.

Left panel is adapted from (Winters and Bader, J Dev Biol, 2013.) and right panel lists various organs with a mesothelial layer and the common molecular signature of mesothelium.

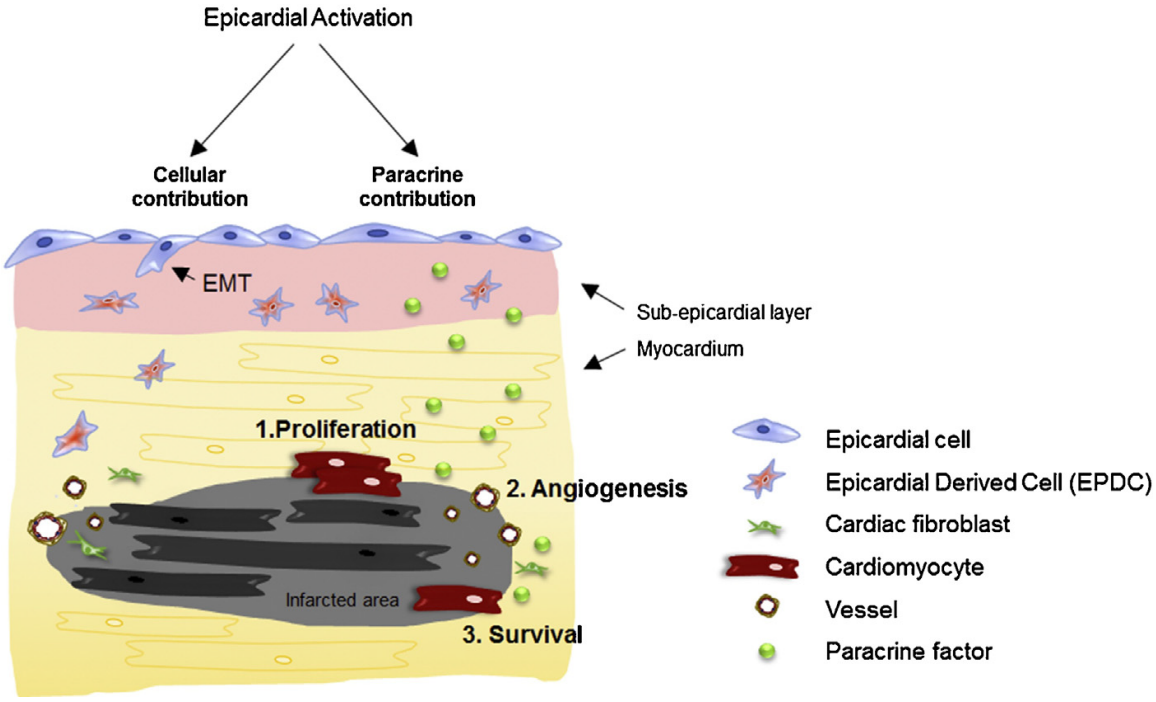

Figure 1.2 Mesothelium activation in the heart.

Epicardium is reactivated after injury and undergoes and epithelial-mesenchymal transition to invade the underyling layer. Upon reactivation, gene expression and plasticity reverts to a state reminiscient of embryoic mesothelium. Adapted from (Smits, Dronkers & Goumans. Pharmacol. Res. 2017.)

References

1. Heidary Rouchi, A. and Mahdavi-Mazdeh, M. (2015) Regenerative Medicine in Organ and Tissue Transplantation: Shortly and Practically Achievable? Int J Organ Transplant Med 6 (3), 93-98.

2. Benjamin, E.J. et al. (2017) Heart Disease and Stroke Statistics-2017 Update: A Report From the American Heart Association. Circulation 135 (10), e146-e603.

3. Sampogna, G. et al. (2015) Regenerative medicine: Historical roots and potential strategies in modern medicine. Journal of Microscopy and Ultrastructure 3 (3), 101-107.

4. Wu, R. et al. (2018) Concise Review: Optimized Strategies for Stem Cell-Based Therapy in Myocardial Repair: Clinical Translatability and Potential Limitation. Stem Cells.

5. Golpanian, S. et al. (2016) Concise Review: Review and Perspective of Cell Dosage and Routes of Administration From Preclinical and Clinical Studies of Stem Cell Therapy for Heart Disease. Stem Cells Transl Med 5 (2), 186-191.

6. Campbell, N.G. and Suzuki, K. (2012) Cell delivery routes for stem cell therapy to the heart: current and future approaches. J Cardiovasc Transl Res 5 (5), 713-726.

7. Murphy, S.V. and Atala, A. (2014) 3D bioprinting of tissues and organs. Nat Biotechnol 32 (8), 773-785.

8. Zhang, Y.S. et al. (2017) 3D Bioprinting for Tissue and Organ Fabrication. Ann Biomed Eng 45 (1), 148-163.

9. Wilm, B. et al. (2005) The serosal mesothelium is a major source of smooth muscle cells of the gut vasculature. Development 132 (23), 5317-5328.

10. Rinkevich, Y. et al. (2012) Identification and prospective isolation of a mesothelial precursor lineage giving rise to smooth muscle cells and fibroblasts for mammalian internal organs, and their vasculature. Nat Cell Biol 14 (12), 1251-1260.

11. Cano, E. et al. (2013) Wt1-expressing progenitors contribute to multiple tissues in the developing lung. Am J Physiol Lung Cell Mol Physiol 305 (4), L322-L332.

12. Winters, N. and Bader, D. (2013) Development of the Serosal Mesothelium. J Dev Biol 1 (2), 64-81.

13. Mutsaers, S.E. (2002) Mesothelial cells: Their structure, function and role in serosal repair. Respirology 7 (3), 171-191.

14. Mutsaers, S.E. (2004) The mesothelial cell. Int J Biochem Cell Biol 36 (1), 9-16.

15. Lua, I. and Asahina, K. (2016) The Role of Mesothelial Cells in Liver Development, Injury, and Regeneration. Gut Liver 10 (2), 166-176.

16. Zeng, B. et al. (2011) Developmental patterns and characteristics of epicardial cell markers Tbx18 and Wt1 in murine embryonic heart. J Biomed Sci 18 (67).

17. Dauleh, S. et al. (2016) Characterisation of Cultured Mesothelial Cells Derived from the Murine Adult Omentum. PLoS One 11 (7), e0158997.

18. Wang, J. et al. (2015) Epicardial regeneration is guided by cardiac outflow tract and Hedgehog signalling. Nature 522 (7555), 226-230.

19. Masters, M. and Riley, P.R. (2014) The epicardium signals the way towards heart regeneration. Stem Cell Res 13 (3 Pt B), 683-692.

20. van Wijk, B. et al. (2012) Cardiac Regeneration from Activated Epicardium. PLoS ONE 7 (9), 1-14.

21. Asahina, K. et al. (2009) Mesenchymal origin of hepatic stellate cells, submesothelial cells, and perivascular mesenchymal cells during mouse liver development. Hepatology 49 (3), 998-1011.

22. Chen, Y.T. et al. (2014) Lineage tracing reveals distinctive fates for mesothelial cells and submesothelial fibroblasts during peritoneal injury. J Am Soc Nephrol 25 (12), 2847-2858.

23. Iyer, D. et al. (2015) Robust derivation of epicardium and its differentiated smooth muscle cell progeny from human pluripotent stem cells. Development 142 (8), 1528-1541.

24. Mellgren, A.M. et al. (2008) Platelet-derived growth factor receptor beta signaling is required for efficient epicardial cell migration and development of two distinct coronary vascular smooth muscle cell populations. Circ Res 103 (12), 1393-1401.

25. Singh, A. et al. (2016) Hippo Signaling Mediators Yap and Taz Are Required in the Epicardium for Coronary Vasculature Development. Cell Rep 15 (7), 1384-1393.

26. Tian, X. et al. (2015) Cellular origin and developmental program of coronary angiogenesis. Circ Res 116 (3), 515-530.

27. Ishii, Y. et al. (2010) BMP signals promote proepicardial protrusion necessary for recruitment of coronary vessel and epicardial progenitors to the heart. Dev Cell 19 (2), 307-316.

28. Watt, A.J. et al. (2004) GATA4 Is Essential for Formation of the Proepicardium and Regulates Cardiogenesis. Proc Natl Acad Sci U S A 101 (34), 12573-12578.

29. Perez-Pomares, J.M. et al. (2002) Origin of coronary endothelial cells from epicardial mesothelium in avian embryos. Int J Dev Biol 46 (8), 1005-1013.

30. Ruiz-Villalba, A. and Pérez-Pomares, J.M. (2012) The expanding role of the epicardium and epicardial-derived cells in cardiac development and disease. Curr Opin Pediatr 24 (5), 569-576.

31. Smits, A.M. et al. (2018) The epicardium as a source of multipotent adult cardiac progenitor cells: Their origin, role and fate. Pharmacol Res 127, 129-140.

32. Di Meglio, F. et al. (2010) Epithelial-mesenchymal transition of epicardial mesothelium is a source of cardiac CD117-positive stem cells in adult human heart. J Mol Cell Cardiol 49 (5), 719-727.

33. Rao, K.S. and Spees, J.L. (2017) Harnessing Epicardial Progenitor Cells and Their Derivatives for Rescue and Repair of Cardiac Tissue After Myocardial Infarction. Curr Mol Biol Rep 3 (3), 149-158.

34. Que, J. et al. (2008) Mesothelium Contributes to Vascular Smooth Muscle and Mesenchyme during Lung Development. Proc Natl Acad Sci U S A 105 (43), 16626-16630.

35. Witty, A.D. et al. (2014) Generation of the epicardial lineage from human pluripotent stem cells. Nat Biotechnol 32 (10), 1026-1035.

CHAPTER 2

BUILDING BLOOD VESSELS WITH VASCULAR PROGENITOR CELLS[1]

[1]Colunga, T. and S. Dalton. 2018. Submitted to *Trends in Molecular Medicine*, 03/21/18.

Abstract

Vascular progenitor cells have been identified from multiple sources and share the ability to generate at least some of the vascular lineages including endothelial cells, smooth muscle cells and pericytes. The therapeutic use for vascular progenitor cells is potentially broad and includes applications relating to stroke, ischemic disease of multiple organs including the heart and in the engineering of whole organs and tissues that require a vascular component. This review summarizes the best characterized sources of vascular progenitor cells and will highlight current progress and future potential for these cells in regenerative medicine and corrective surgery.

Clinical Significance of Vascular Progenitor Cells

Vascular disease can be attributed to a number of factors and impacts millions of patients with a broad range of clinical disorders that affect multiple organs. In some cases, **vasculopathies** (see Glossary) arise as a consequence of other conditions. For example, peripheral vascular disease is frequently linked to complex metabolic diseases such as diabetes. Diabetes also increases the risk of amputation for patients dealing with high blood pressure-induced peripheral artery disease which is caused by a narrowing of the artery and reduction of blood flow [1]. Other conditions such as stroke or coronary, renal and pulmonary disease can result from blood pressure dysregulation, reduction of blood flow and vascular occlusion [2-5]. Over 370 million people worldwide suffer from diabetes and costs related to cardiovascular disease and stroke is currently >$300 billion annually and will exceed $1 trillion by 2035 [6, 7]. This represents a massive public health problem and although pharmacological treatments and surgical reconstruction of

large vessels are commonly used to minimize disease progression, surgical replacement of vessels smaller than 5mm in diameter remains problematic [8, 9]. Vascular repair is also a critical factor in the recovery of patients with traumatic injury which can often result in amputation and high mortality rates [10]. If synthetic, cellularized vessels can be generated that retain biological function over extended periods of time without clotting or promoting an inflammatory response, this would constitute a major advance in the treatment of vasculopathy and traumatic injury.

Vascular disease is frequently associated with occlusion events that restrict or completely blocks blood flow around the body. Such blockages lead to rapid inflammation, cell death, fibrosis and chronic functional decline [11, 12]. Depending on diagnosis and patient history, treatment of vascular occlusion includes pharmacological intervention, **angioplasty** and **vascular bypass** surgery. While angioplasty is generally effective it is susceptible to **stenosis** and is only a suitable option for a subset of patients [13]. Alternatively, autologous sections of the saphenous vein or thoracic artery can be used for bypass surgery but availability of this material is limited. Synthetic grafts have also been used but they only have efficacy over short time-frames and succumb to occlusion and inflammation; this is particularly problematic in small diameter vessels [14-16]. A potential solution to this problem is to seed cells on biological or non-biological scaffolds to generate tissue engineered vascular grafts (TEVGs). While this general approach has been attempted using combinations of smooth muscle cells, endothelial cells and mesenchymal stem cells (MSCs) success has been limited [17-19]. For example, infiltration of the endothelial layer by smooth muscle cells often causes

occlusion and inflammation resulting in graft failure. An alternative 'cell' approach is therefore required to alleviate problems associated with TEVGs. Use of vascular progenitor cells with significant developmental plasticity and migratory capacity is a potential solution. This issue will be addressed by discussing the developmental origins and biological properties of different vascular progenitor cells. We will then describe the progenitor cells that hold most promise for clinical use and strategies of cell delivery, including the direct transplantation of cells into diseased and injured tissue and the use of vascular progenitor cells in TEVGs. Lastly, we will cover future directions the field could take by focusing on the interface between tissue engineering and stem cell biology.

Developmental Origins of Vascular Progenitor Cells

Almost all cells with vascular potential arise from the mesoderm lineage. The first vascular progenitors identified during human **embryogenesis** give rise to blood islands - small mesoderm-derived clusters of cells in the yolk sac that contribute to the earliest vascular structure, the primitive capillary plexus [20-23]. This plexus is void of supporting stromal cells and consists of endothelium derived from the distal cells of the blood island while the inner hematopoietic population gives rise to blood cells [22]. Blood islands are not known to persist throughout development and efforts to isolate and culture this population in vitro has not been reported. Thus, their utility for cellular therapy or tissue engineering is questionable.

Hemangioblasts and mesoangioblasts are two other cell populations that give rise to blood vessels during early post-gastrulation development. Postnatally, both cell types

disperse into multiple tissues such as the heart and bone marrow where they contribute to new blood vessel generation and can be isolated for long-term culture [24-27]. Both cell types also express vascular endothelial growth factor receptor 2/fetal liver kinase 1 (VEGFR2/Flk1), while CD34 with CD45 are associated with hemangioblasts [25, 27]. Hemangioblasts have the inherent ability to give rise to blood cells and endothelium but are not considered a direct progenitor of vascular smooth muscle cells (VSMCs) or pericytes (Pcs) [28]. Mesoangioblasts do not directly generate blood cells but contribute to endothelium, VSMCs, Pcs and other non-vascular cell types [25, 26, 29]. The developmental contribution of mesangioblasts and hemangioblasts to blood vessel formation remains unchallenged but their potential use as cell therapeutics is less clear [26, 30].

Resident Adult Vascular Progenitors

Coelomic organs and body cavities are lined on their outside surfaces by a layer of epithelial cells called mesothelium [31]. The best characterized mesothelial layer is the epicardium, which forms around the myocardium [32]. Various mesothelium lineage-tracing studies in mouse gut, liver, lung, kidney and heart have reported contrasting results in terms of vascular contribution by the mesothelium lineage. In some studies mesothelium contribution to the vasculature has been restricted to VSMCs and Pcs while others show strong endothelial contribution [33-36]. This conflict could be representative of technical issues relating to the choice of Cre-drivers or, due to differences in the role of mesothelium in vascular development of these organs. Besides vascular contribution, mesothelium-derived cells can give rise to hepatic stellate cells, MSCs, fibroblasts,

adipocytes, chondrocytes and osteocytes [37-39]. Under normal physiological conditions, mesothelium in the adult participates in organ **homeostasis** and is **quiescent** but can be reactivated following injury [39, 40]. This is exemplified in the heart where a subpopulation of epicardium cells migrates into the sub-epicardial and myocardial layers as they transform into migratory epicardial-derived cells (EPDCs). In the underlying tissue, EPDCs play a role in tissue repair and/or regeneration at multiple levels [41, 42]. First, by promoting **neo-vascularization** by directly contributing to VSMCs and perivascular Pcs in new vessels and second, by releasing signaling molecules that promote repair and finally, by deposition of extracellular matrix (ECM) [43, 44]. In the heart, cells of the mesothelium lineage are a source of resident vascular progenitors with potential therapeutic implications [40]. Primary EPDC isolation (Figure 1) is highly invasive and maintenance of vascular potential in vitro is limited which restricts their potential clinical utility [44].

Primary Endothelium and Endothelial Progenitors

Blood vessels are typically organized so that VSMCs surround the endothelium in arteries and veins while perivascular Pcs line endothelial cells of the microvasculature. Endothelial cells (ECs) occupy the **lumenal** side of vessels and express von Willebrand factor, CD31 and CD144 on their surface and have acetylated LDL uptake activity [45, 46]. ECs function as a selective barrier in blood vessels that modulate the diffusion of white blood cells and solutes across to the surrounding tissue and for selective transport of waste products and CO_2 from the surrounding tissue into the bloodstream. This selective barrier function is conferred by tight junctions between neighboring endothelial

cells and by the presence of pores in a subset of ECs known as fenestrated endothelium [46-48]. Human umbilical vein endothelial cells (HUVECs) and microvascular endothelium (MVECs) are two of the most commonly used primary endothelial sources for TEVG construction but they have practical limitations. Mertsching et al. showed that although MVECs can successfully reseed decellularized vasculature in vitro, the resulting vessels clot shortly after transplantation into patients [49]. Coupled with inflammation, this constitutes a major problem encountered following transplantation of vessels, particularly those of small-medium diameter (<5mm) [50, 51]. These problems have forced researchers to rethink and explore other cell sources such as endothelial progenitor cells (EPCs) that could have greater developmental plasticity and may not be subject to these problems.

Circulating EPCs (Figure 1) are one prospective endothelial cell source because of their availability from peripheral blood mononuclear cell fractions [52, 53]. Coupled with in vitro colony forming and clonogenic potential, this class of EPCs are commonly referred to as endothelial colony-forming cells (ECFCs) [54]. Much controversy surrounds the definition and developmental origins of circulating ECFCs but most evidence points towards them having a hematopoietic origin [55, 56]. ECFCs promote vascularization by contributing to the endothelium of newly-formed blood vessels following injury and can modulate the regenerating vascular microenvironment through the release of **paracrine** factors [57, 58]. As an example of the latter, ECFCs reduce apoptosis and astrocytic scar formation and increase capillary density in a mouse neonatal hypoxic ischemic encephalopathy model. No clear evidence of ECFC-derived endothelial

vessel contribution was observed in this study, however [57]. In a rat cerebral ischemia model, Moubarik et al. also report a reduction of apoptosis coupled with increased capillary density and functional neurological recovery but saw no evidence for neo-vessel contribution by ECFCs [58]. Supporting a direct role in neo-vascularization, Prasain et al. reported that ECFCs directly contribute to vascular repair in mice using hind-limb ischemia and oxygen-induced retinopathy models [59]. In a therapeutic context, ECFCs have therapeutic potential by working through different mechanisms. Further work is required to establish their full utility and mechanism of action.

Mesenchymal Stem Cells

In vivo equivalents of MSCs (Figure 1) are considered to be widely present throughout the body including the vasculature, adipose tissue, bone marrow, placenta and cord blood. These cells are characterized by the expression of CD90, CD166 and CD29 but do not express common vascular progenitor markers such as VEGFR2/Flk1 and CD34 [60, 61]. While displaying multipotency in vitro and in vivo, their tissue location and developmental origins are hotly debated and intertwined with perivascular Pcs [62, 63]. Despite a propensity for differentiation into non-vascular lineages, MSCs have been shown to perform a support role in **angiogenesis** following myocardial infarction and hind-limb ischemia [12, 64]. In these latter contexts, MSCs function by a paracrine signaling mechanism that supports endothelial cell growth and differentiation but also promote the activity of Pc and VSMC populations [65]. MSCs also serve as immune-modulators by suppressing the host immune system thereby lowering rejection incidences following **allogeneic** transplantation [66, 67]. MSCs are among the few cell types that

have progressed to clinical trial status for cell therapy. The TAC-HFT and PROMETHEUS clinical trials focused on the contributions of bone marrow-derived MSCs in patients diagnosed with chronic ischemic cardiomyopathy [68, 69]. In vitro, this population generates vascular lineages such as endothelium and VSMCs but neither trial reported the contribution of MSCs to new blood vessel formation at or near the injection site. MSCs did however, promote increased left ventricle ejection fraction (LVEF) and suppressed scar tissue formation via paracrine mechanisms [68, 69]. While these individual studies look promising, a recent meta-analysis showed that MSCs have no clear clinical benefit for treatment of myocardial infarction [70]. More studies are required to resolve this issue and to define in greater detail the mechanism of action by which MSCs function. In addition to being a therapeutic option for tissue damage, MSCs have potential utility in conjunction with primary endothelial cells in the engineering of TEVGs [71].

Pluripotent Stem Cells

Human pluripotent stem cells (hPSCs) (Figure 1) can be cultured indefinitely as a self-renewing population and differentiated into all adult lineages [72-74]. This gives them many advantages and increased utility when compared to other multipotent cells that often have limited self-renewal capacity and restricted developmental potential [73, 74]. The ability of hPSCs to generate endothelium, VSMCs and Pcs by directed differentiation provides the field with a cell source that can, in principal, generate an unlimited supply of vascular lineages [35, 45, 59, 74-76]. Molecular and functional analysis reveal that hPSC-derived endothelium and VSMCs are analogous to their

counterparts derived from tissue but now their clinical utility must be demonstrated [45, 47, 77]. Kusuma et al. generated an "early vascular cell" by directed differentiation that successfully gave rise to self-assembling endothelium and Pcs into capillary-like networks in vitro and in vivo after subcutaneous implantation in mice [76]. Whether these cells are suitable for clinical use is unclear because they seem to represent an early mesoderm cell type capable of broad differentiation capacity. Park et al. conducted a small scale hind-limb ischemia study utilizing hPSC-derived EPCs by modulating important cell signaling networks in a directed differentiation protocol followed by cell sorting to obtain an enriched population [78]. Despite lower than ideal differentiation efficiency, clinical utility was shown by their incorporation into newly formed blood vessels and release of angiogenic cytokines [78]. Contribution of hPSC-derived endothelium is critical but blood vessels also require VSMCs or Pcs for structural integrity and support. While these cells have potential use in a range of applications, a hPSC-derived multipotent vascular progenitor that can form all vascular lineages has not been reported.

Cellular Therapy – Moving Beyond the Cell?

Restoration of blood perfusion after stroke, ischemic disease or traumatic injury is critical to minimize long-term tissue damage. To mitigate these problems direct cellular injection of EPCs into the rodent myocardium has been attempted with numerous beneficial outcomes reported [79, 80]. Administration of EPCs coupled with pharmacological treatment also increases microvascular density and improves neurological function in diabetic ischemic stroke [81]. Unlike these examples however,

the vast majority of translational research surrounding vascular progenitor utility is still in the proof of concept phase and has yet to move into large animal models where long-term efficacy must be demonstrated [82, 83]. Compelling data to support clinical utility of vascular progenitors is probably 5-10 years away but, as described, there are some encouraging reports that must be corroborated and translated into a clinical product.

As an alternative strategy to using exogenous cells to build vascular networks, pro-angiogenic components such as RNA and protein can be delivered to the site of injury. Zangi et al. showed that injection of a soluble synthetic VEGF mRNA after myocardial infarction improved functional cardiac readouts and promoted recruitment of resident EPDCs to promote neo-vascularization around the infarcted area [84]. **Exosomes** secreted by vascular progenitors are also another potential tool to promote vasculogenesis [85]. *Trans*-differentiation of resident cells along the vascular lineage in vivo is another approach being explored to promote tissue regeneration. Using nanotechnology Gallego-Perez et al. recently showed that dermal cells could be *trans*-differentiated to ECs using nanoporation to deliver reprogramming factors [86]. When this technology was applied to a hind-limb ischemia model, blood perfusion increased due to the formation of nascent blood vessels derived from trans-differentiated cells [86]. While these results are exciting and still in the exploratory stage, they raise the possibility that manipulation of cell identity in vivo could be a viable approach for cell replacement therapy.

Barriers and Challenges to Making Vascular Grafts

TEVGs are comprised of a natural or fabricated scaffold onto which cells can be seeded. TEVGs have potential utility in the treatment of a wide-range of vascular diseases including myocardial infarction, peripheral artery and venous disease, atherosclerosis, vascular aneurisms and stroke (Figure 2, Key Figure). While the introduction of large diameter (>5mm) grafts have had some success, replacement of smaller vessels has been more problematic [16, 19, 87]. **Autologous** grafts have high rates of failure in the first 5-10 years post-surgery and the amount of material available is limited [14, 15]. The situation is also complicated by the donor's clinical condition that will impact tissue quality (e.g. diabetes and age) [15]. Complications associated with grafts of <5mm in diameter are generally attributed to inflammation, stenosis and neo-tissue hyperplasia mediated by macrophage infiltration [14, 15, 51, 88]. The challenges to engineer TEVGs that function reliably over extended periods (>10 years) is heavily impacted by the physical demands placed on such bio-constructs. Optimal tensile strength, mechanical flexibility, the ability to vaso-constrict and vaso-dilate and a consideration of burst pressures are all factored into vessel design making it a challenging process [8, 50, 89-91]. These mechanical properties are heavily influenced by choice of material and cell source and each choice appears to have its own advantages and disadvantages [50, 87, 88, 92-94]. For example, TEVGs seeded with MSCs effectively cellularize and remodel following transplantation but remain susceptible to thrombosis [87, 92]. Thus, there is an urgent need to develop new TEVG technologies that solve these barriers.

Bioengineering of Scaffolds for Vascular Grafts

A range of progenitor and differentiated cells have been described that are currently in use for TEVG development. Their use in conjunction with biological and fabricated scaffolds for development of TEVGs will now be discussed, beginning with acellular biological scaffolds.

Decellularized vascular scaffolds have been prepared from various vascular sources and anatomical locations to serve as a test-bed for clinical development and therapeutic applications [95-98]. Decellularized scaffolds are a desirable platform on which to base TEVGs as they retain a native ECM onto which vascular lineages can be assembled [99-101]. The decellularization of vessel scaffolds requires detergents and enzymes and the cellularization step optimally requires a bioreactor to control growth conditions and to modulate perfusion rates [96, 97, 99]. Decellularized scaffolds seeded with vascular cells have been shown to function following anastomosis in animal models but still remain susceptible to thrombosis and failure in the acute stage following transplantation [102].

While the development of next-generation decellularized constructs is ongoing, tissue engineers have developed fabricated scaffolds to overcome problems associated with existing TEVGs. As a way to reproduce biological scaffolds, but with the advantage of customizing vessel properties, natural components such as collagen, gelatin and fibrin are used for scaffold fabrication [93, 103]. These proteins can be crosslinked to varying degrees to obtain constructs with different properties for different applications. These

materials are commonly used in conjunction with 3D printing and electrospinning technologies to generate scaffolds that can be cellularized with progenitors or mixtures of mature vascular cells.

As an alternative to natural materials that are found in blood vessel walls, tissue engineers have adopted the use of synthetic polymers in 3D printing and electrospinning applications (Figure 2) [89, 104-106]. Polymers such as poly-lactic acid, poly-glycolyic acid and ε-caprolactone are used alone or in combination to generate TEVGs [50, 87, 88]. These polymers can generate TEVGs with varying degrees of porosity, tensile strength and flexibility and can accommodate different cell types that can be loaded with growth factors and small molecules that promote cellular maturation. These technologies can be used for the fabrication of precise, personalized constructs in contrast to decellularized constructs which are more limited in shape, size and branching.

3D printing and electrospinning matrices are frequently designed to orientate cells individually or in layers to form vessel structures that will support blood flow following transplantation [50, 92, 104-106]. These scaffolds are made with high technical specifications and can incorporate multiple materials assembled into multiple layers that give different physical and biochemical characteristics. The rationale in the design of TEVGs is to facilitate assembly of cells on the tunica intima and the tunica externa and throughout the tunica media by introducing porous materials that allow for cell migration, attachment and maturation [88, 105-108]. Potential for this technology is underscored by recent work by Mirabella and co-workers who used transplanted TEVGs comprised of

3D printed grafts seeded with HUVECs [105]. Here, grafts significantly improved blood perfusion and provided a therapeutic benefit in hind-limb ischemia and myocardial infarction models.

Concluding Remarks

Vascular disease is one of the most significant medical problems facing our society. A potentially effective way to address this problem is to utilize stem cell biology with tissue engineering. In this review, we discussed how vascular progenitors can be used in conjunction with scaffolds to generate blood vessels that can replace diseased or damaged vasculature. The introduction of new materials from an engineering perspective combined with the derivation of vascular progenitor cells, that have developmental plasticity and which can assemble into functional vessels, are likely to play an important role in this area. When choosing a vascular progenitor for cellular therapy or tissue engineering, a multitude of parameters including cell type, cell number, delivery method (i.e. use of scaffold) and location, patient diagnosis, age and paracrine versus autocrine factors must be considered. The ultimate goal of manufacturing an 'off-the-shelf' TEVG for vascular disease and corrective surgery has not yet been achieved (see Outstanding Questions). However, stem cell technology, materials science and bioengineering in the future offer a potential solution to this biomedical problem.

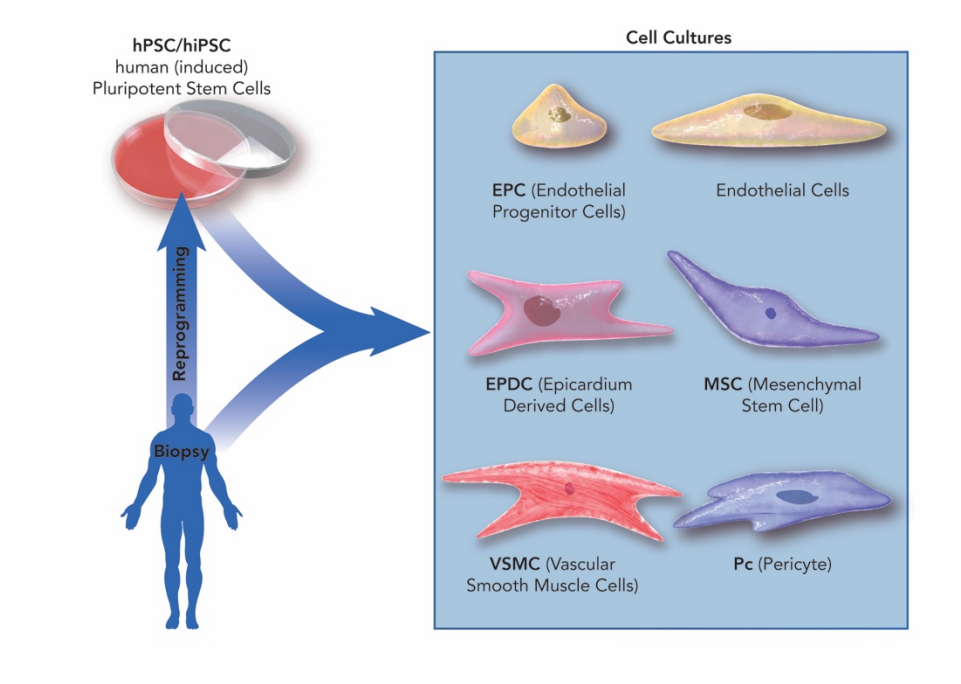

Figure 2.1. Cell types used for vascular repair and for vascular engineering applications.

Primary cells from individuals can be used directly or following cellular reprogramming to generate vascular cell types. Reprogrammed cells offer a potentially unlimited supply of autologous cells for implantation which could minimize rejection. Primary cells such as EPCs, endothelial cells, VSMCs, Pcs and MSCs can be routinely harvested for expansion and use in cellular therapy and tissue engineering applications.

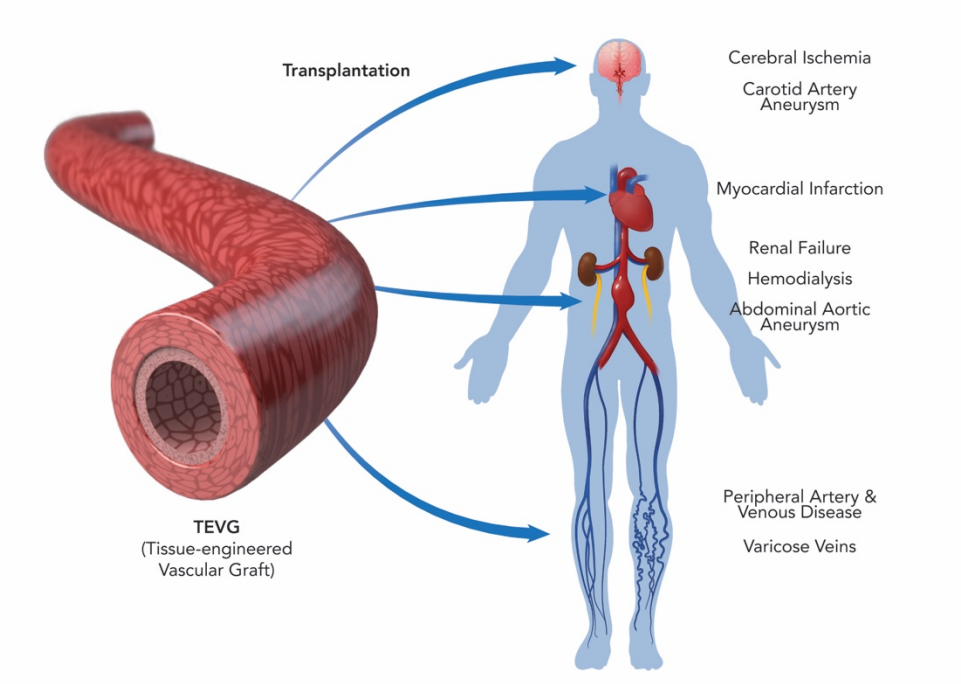

Figure 2.2. Tissue engineered vascular grafts and their potential use in vascular engineering.

TEVG scaffolds can be generated from biological material such as decellularized arteries and veins or from fabricated materials that can be assembled into scaffolds using 3D-printing or electrospinning technology. These scaffolds are then seeded with vascular progenitor cells for the generation of transplantable TEVGs.

Glossary

Allogeneic: relates to cells or other biological material that are from the same species but transplanted into other individuals (e.g. bone marrow transplantations).

Angiogenesis: formation of new blood vessels that branch-off from existing ones.

Angioplasty: surgical procedure to open blocked arteries. This procedure is frequently used to clear coronary vessels.

Autologous: transplantation of cells or other biological material that are derived from the recipient.

Embryogenesis: early development in humans that covers the first eight weeks post fertilization and encompasses formation of the three germ layers.

Exosomes: membrane bound vesicles released by cells. These vesicles carry cargo such as growth factors, proteins, microRNA and lipids that impact function of other cell types.

Homeostasis: the process by which tissues and organs self-regulate to maintain function.

Lumenal: the inner cavity of a blood vessel that is typically covered with endothelium and is the conduit for flow of blood cells.

Neo-vascularization: formation of new blood vessels in areas that previously had no vascular networks or in tissues that experienced trauma (e.g. myocardial infarction).

Paracrine: release of cell signaling molecules, growth factors, cytokines and chemokines by one cell that only influence nearby or distant cells.

Quiescent: a cellular state that is marked by temporary exit from the cell cycle but allows for re-entry to actively divide and proliferate.

Stenosis: the narrowing of a blood vessel causing restricted blood flow. In tissue engineered vascular grafts this can be caused by calcification and inflammation related to immune cell invasion.

Vascular Bypass: surgical procedure typically associated with blockage or narrowing due to plaque build-up. Arteries or veins from another part of the body or synthetic vessels are grafted to bypass the blocked area to restore blood flow.

Vasculopathies: any number of diseases or defects of the blood vessels that leads to functional decline.

Highlights

- Vascular progenitors are a potential cell source for tissue engineering and tissue repair
- Multiple problems exist in relation to vascular graft technology
- Use of vascular progenitors instead of fully differentiated cell types is a feasible approach to solve some problems associated with vascular engineering
- Biological and fabricated scaffolds are viable alternatives that can be cellularized for the purpose of generating transplantable vascular grafts

Outstanding Questions

- Which cells are going to prove of most utility for vascular graft engineering?
- Will pre-seeded TEVGs have more clinical utility than acellular grafts?
- Can problems associated with current vascular graft approaches be overcome with new materials and alternate cell sources?
- Is an off-the-shelf cellular TEVG attainable?

References

1. Quilici, M.T. et al. (2016) Risk Factors for Foot Amputation in Patients Hospitalized for Diabetic Foot Infection. J Diabetes Res 2016, 8931508.

2. Karayiannides, S. et al. (2018) High overall cardiovascular risk and mortality in patients with atrial fibrillation and diabetes: A nationwide report. Diab Vasc Dis Res 15 (1), 31-38.

3. Dinesh Shah, A. et al. (2015) Type 2 diabetes and incidence of a wide range of cardiovascular diseases: a cohort study in 1·9 million people. The Lancet 385 Suppl 1, S86-S86.

4. Fowkes, F.G.R. et al. (2013) Comparison of global estimates of prevalence and risk factors for peripheral artery disease in 2000 and 2010: a systematic review and analysis. The Lancet 382 (9901), 1329-1340.

5. Muthiah, A. et al. (2017) A study on diabetic foot and its association with peripheral artery disease. Int Surg J 4 (4), 1217-1221.

6. Benjamin, E.J. et al. (2017) Heart Disease and Stroke Statistics-2017 Update: A Report From the American Heart Association. Circulation 135 (10), e146-e603.

7. Cardiovascular Disease: A Costly Burden for America, Projections Through 2035, American Heart Association, 2017, pp. 1-16.

8. Nezarati, R.M. et al. (2015) Electrospun vascular grafts with improved compliance matching to native vessels. J Biomed Mater Res B Appl Biomater 103 (2), 313-323.

9. Kurobe, H. et al. (2015) Development of small diameter nanofiber tissue engineered arterial grafts. PLoS One 10 (4), e0120328.

10. Tan, T.W. et al. (2011) Limb outcome and mortality in lower and upper extremity arterial injury: a comparison using the National Trauma Data Bank. Vasc Endovascular Surg 45 (7), 592-597.

11. Samuel, R. et al. (2015) Vascular diseases await translation of blood vessels engineered from stem cells. Sci Transl Med 7 (309), 309rv6.

12. Koch, J.M. et al. (2016) Mesenchymoangioblast-derived mesenchymal stromal cells inhibit cell damage, tissue damage and improve peripheral blood flow following hindlimb ischemic injury in mice. Cytotherapy 18 (2), 219-228.

13. Byrne, R.A. et al. (2017) Coronary balloon angioplasty, stents, and scaffolds. The Lancet 390 (10096), 781-792.

14. Deb, S. et al. (2012) Radial artery and saphenous vein patency more than 5 years after coronary artery bypass surgery: results from RAPS (Radial Artery Patency Study). J Am Coll Cardiol 60 (1), 28-35.

15. Tranbaugh, R.F. et al. (2017) Coronary Artery Bypass Graft Surgery Using the Radial Artery, Right Internal Thoracic Artery, or Saphenous Vein as the Second Conduit. Ann Thorac Surg 104 (2), 553-559.

16. Hibino, N. et al. (2010) Late-term results of tissue-engineered vascular grafts in humans. J Thorac Cardiovasc Surg 139 (2), 431-6, 436 e1-2.

17. Villalona, G.A. et al. (2010) Cell-Seeding Techniques in Vascular Tissue Engineering. Tissue Eng Part B Rev 16 (3), 341-350.

18. Lee, Y.-U. et al. (2016) Rational design of an improved tissue-engineered vascular graft: determining the optimal cell dose and incubation time. Regen Med 11 (2), 159-167.

19. Drews, J.D. et al. (2017) Tissue-engineered vascular grafts for congenital cardiac disease: Clinical experience and current status. Trends Cardiovasc Med 27 (8), 521-531.

20. Kovacic, J.C. and Boehm, M. (2009) Resident vascular progenitor cells: an emerging role for non-terminally differentiated vessel-resident cells in vascular biology. Stem Cell Res 2 (1), 2-15.

21. McLeod, D.S. et al. (2012) From blood islands to blood vessels: morphologic observations and expression of key molecules during hyaloid vascular system development. Invest Ophthalmol Vis Sci 53 (13), 7912-7927.

22. Potente, M. and Makinen, T. (2017) Vascular heterogeneity and specialization in development and disease. Nat Rev Mol Cell Biol 18 (8), 477-494.

23. Goldie, L.C. et al. (2008) Embryonic vasculogenesis and hematopoietic specification. Organogenesis 4 (4), 257-263.

24. Pelosi, E. et al. (2002) Identification of the hemangioblast in postnatal life. Blood 100 (9), 3203-3208.

25. Azzoni, E. et al. (2014) Hemogenic endothelium generates mesoangioblasts that contribute to several mesodermal lineages in vivo. Development 141 (9), 1821-1834.

26. Galvez, B.G. et al. (2008) Cardiac mesoangioblasts are committed, self-renewable progenitors, associated with small vessels of juvenile mouse ventricle. Cell Death Differ 15 (9), 1417-1428.

27. Pelosi, E. et al. (2012) Human haemato-endothelial precursors: cord blood CD34+ cells produce haemogenic endothelium. PLoS One 7 (12), e51109.

28. Stefanska, M. et al. (2014) Smooth muscle cells largely develop independently of functional hemogenic endothelium. Stem Cell Res 12 (1), 222-232.

29. Minasi, M.G. et al. (2002) The meso-angioblast: a multipotent, self-renewing cell that originates from the dorsal aorta and differentiates into most mesodermal tissues. Development 129 (11), 2773-2783.

30. Galli, D. et al. (2005) Mesoangioblasts, vessel-associated multipotent stem cells, repair the infarcted heart by multiple cellular mechanisms: a comparison with bone marrow progenitors, fibroblasts, and endothelial cells. Arterioscler Thromb Vasc Biol 25 (4), 692-697.

31. Winters, N. and Bader, D. (2013) Development of the Serosal Mesothelium. J Dev Biol 1 (2), 64-81.

32. Munoz-Chapuli, R. et al. (2002) The epicardium and epicardial-derived cells: Multiple functions in cardiac development. Rev Esp Cardiol (Engl Ed) 55 (10), 1070-1082.

33. Wilm, B. et al. (2005) The serosal mesothelium is a major source of smooth muscle cells of the gut vasculature. Development 132 (23), 5317-5328.

34. Volz, K.S. et al. (2015) Pericytes are progenitors for coronary artery smooth muscle. Elife 4, e10036.

35. Rinkevich, Y. et al. (2012) Identification and prospective isolation of a mesothelial precursor lineage giving rise to smooth muscle cells and fibroblasts for mammalian internal organs, and their vasculature. Nat Cell Biol 14 (12), 1251-1260.

36. van Wijk, B. et al. (2012) Cardiac Regeneration from Activated Epicardium. PLoS ONE 7 (9), 1-14.

37. Lua, I. and Asahina, K. (2016) The Role of Mesothelial Cells in Liver Development, Injury, and Regeneration. Gut Liver 10 (2), 166-176.

38. Lansley, S.M. et al. (2011) Mesothelial cell differentiation into osteoblast- and adipocyte-like cells. J Cell Mol Med 15 (10), 2095-2105.

39. Chen, Y.T. et al. (2014) Lineage tracing reveals distinctive fates for mesothelial cells and submesothelial fibroblasts during peritoneal injury. J Am Soc Nephrol 25 (12), 2847-2858.

40. Bollini, S. et al. (2014) Re-activated adult epicardial progenitor cells are a heterogeneous population molecularly distinct from their embryonic counterparts. Stem Cells Dev 23 (15), 1719-1730.

41. Porrello, E.R. et al. (2011) Transient regenerative potential of the neonatal mouse heart. Science 331 (6020), 1078-1080.

42. Kramann, R. et al. (2015) Perivascular Gli1+ progenitors are key contributors to injury-induced organ fibrosis. Cell Stem Cell 16 (1), 51-66.

43. Reus, T.L. et al. (2016) Secretome from resident cardiac stromal cells stimulates proliferation, cardiomyogenesis and angiogenesis of progenitor cells. Int J Cardiol 221, 396-403.

44. Perez-Pomares, J.M. et al. (2002) Origin of coronary endothelial cells from epicardial mesothelium in avian embryos. Int J Dev Biol 46 (8), 1005-1013.

45. Patsch, C. et al. (2015) Generation of vascular endothelial and smooth muscle cells from human pluripotent stem cells. Nat Cell Biol 17 (8), 994-1003.

46. Urich, E. et al. (2012) Transcriptional profiling of human brain endothelial cells reveals key properties crucial for predictive in vitro blood-brain barrier models. PLoS One 7 (5), e38149.

47. Appelt-Menzel, A. et al. (2017) Establishment of a Human Blood-Brain Barrier Co-culture Model Mimicking the Neurovascular Unit Using Induced Pluri- and Multipotent Stem Cells. Stem Cell Reports 8 (4), 894-906.

48. Satchell, S.C. and Braet, F. (2009) Glomerular endothelial cell fenestrations: an integral component of the glomerular filtration barrier. Am J Physiol Renal Physiol 296 (5), F947-F956.

49. Mertsching, H. et al. (2009) Generation and transplantation of an autologous vascularized bioartificial human tissue. Transplantation 88 (2), 203-210.

50. Zhou, M. et al. (2014) Development and in vivo evaluation of small-diameter vascular grafts engineered by outgrowth endothelial cells and electrospun chitosan/poly(epsilon-caprolactone) nanofibrous scaffolds. Tissue Eng Part A 20 (1-2), 79-91.

51. Hibino, N. et al. (2015) The innate immune system contributes to tissue-engineered vascular graft performance. FASEB J 29 (6), 2431-2438.

52. Peichev, M. et al. (2000) Expression of VEGFR-2 and AC133 by circulating human CD34(+) cells identifies a population of functional endothelial precursors. Blood 95 (3), 952-958.

53. Takayuki Asahara, a. et al. (1997) Isolation of Putative Progenitor Endothelial Cells for Angiogenesis. Science 275 (5302), 964-966.

54. Ingram, D.A. et al. (2004) Identification of a novel hierarchy of endothelial progenitor cells using human peripheral and umbilical cord blood. Blood 104 (9), 2752-2760.

55. Patel, J. et al. (2016) Concise Review: Functional Definition of Endothelial Progenitor Cells: A Molecular Perspective. Stem Cells Transl Med 5 (10), 1302-1306.

56. Chao, H. and Hirschi, K.K. (2010) Hemato-vascular origins of endothelial progenitor cells? Microvasc Res 79 (3), 169-173.

57. Grandvuillemin, I. et al. (2017) Long-Term Recovery After Endothelial Colony-Forming Cells or Human Umbilical Cord Blood Cells Administration in a Rat Model of Neonatal Hypoxic-Ischemic Encephalopathy. Stem Cells Transl Med 6 (11), 1987-1996.

58. Moubarik, C. et al. (2011) Transplanted late outgrowth endothelial progenitor cells as cell therapy product for stroke. Stem Cell Rev 7 (1), 208-220.

59. Prasain, N. et al. (2014) Differentiation of human pluripotent stem cells to cells similar to cord-blood endothelial colony-forming cells. Nat Biotechnol 32 (11), 1151-1157.

60. Lv, F.J. et al. (2014) Concise review: the surface markers and identity of human mesenchymal stem cells. Stem Cells 32 (6), 1408-1419.

61. Holley, R.J. et al. (2015) Comparative quantification of the surfaceome of human multipotent mesenchymal progenitor cells. Stem Cell Reports 4 (3), 473-488.

62. Sacchetti, B. et al. (2016) No Identical "Mesenchymal Stem Cells" at Different Times and Sites: Human Committed Progenitors of Distinct Origin and Differentiation Potential Are Incorporated as Adventitial Cells in Microvessels. Stem Cell Reports 6 (6), 897-913.

63. Blocki, A. et al. (2013) Not all MSCs can act as pericytes: functional in vitro assays to distinguish pericytes from other mesenchymal stem cells in angiogenesis. Stem Cells Dev 22 (17), 2347-2355.

64. Yao, Y. et al. (2015) Paracrine action of mesenchymal stem cells revealed by single cell gene profiling in infarcted murine hearts. PLoS One 10 (6), e0129164.

65. Evensen, L. et al. (2009) Mural cell associated VEGF is required for organotypic vessel formation. PLoS One 4 (6), e5798.

66. Kimbrel, E.A. et al. (2014) Mesenchymal stem cell population derived from human pluripotent stem cells displays potent immunomodulatory and therapeutic properties. Stem Cells Dev 23 (14), 1611-1624.

67. Bartholomew, A. et al. (2002) Mesenchymal stem cells suppress lymphocyte proliferation in vitro and prolong skin graft survival in vivo. Exp Hematol 30 (1), 42-48.

68. Karantalis, V. et al. (2014) Autologous mesenchymal stem cells produce concordant improvements in regional function, tissue perfusion, and fibrotic burden when administered to patients undergoing coronary artery bypass grafting: The Prospective Randomized Study of Mesenchymal Stem Cell Therapy in Patients Undergoing Cardiac Surgery (PROMETHEUS) trial. Circ Res 114 (8), 1302-1310.

69. Heldman, A.W. et al. (2014) Transendocardial mesenchymal stem cells and mononuclear bone marrow cells for ischemic cardiomyopathy: the TAC-HFT randomized trial. JAMA 311 (1), 62-73.

70. Gyongyosi, M. et al. (2015) Meta-Analysis of Cell-based CaRdiac stUdiEs (ACCRUE) in patients with acute myocardial infarction based on individual patient data. Circ Res 116 (8), 1346-1360.

71. Fayol, D. et al. (2013) Design of biomimetic vascular grafts with magnetic endothelial patterning. Cell Transplant 22 (11), 2105-2118.

72. Thomson, J.A. et al. (1998) Embryonic Stem Cell Lines Derived from Human Blastocysts. Science 282 (5391), 1145-1147.

73. Loh, K.M. et al. (2016) Mapping the Pairwise Choices Leading from Pluripotency to Human Bone, Heart, and Other Mesoderm Cell Types. Cell 166 (2), 451-467.

74. Drukker, M. et al. (2012) Isolation of primitive endoderm, mesoderm, vascular endothelial and trophoblast progenitors from human pluripotent stem cells. Nat Biotechnol 30 (6), 531-542.

75. Marchand, M. et al. (2014) Concurrent generation of functional smooth muscle and endothelial cells via a vascular progenitor. Stem Cells Transl Med 3 (1), 91-97.

76. Kusuma, S. et al. (2013) Self-organized vascular networks from human pluripotent stem cells in a synthetic matrix. Proc Natl Acad Sci U S A (31), 12601-12606.

77. Hill, K.L. et al. (2010) Human embryonic stem cell-derived vascular progenitor cells capable of endothelial and smooth muscle cell function. Exp Hematol 38 (3), 246-257 e1.

78. Park, S.W. et al. (2010) Efficient differentiation of human pluripotent stem cells into functional CD34(+) progenitor cells by combined modulation of the MEK/ERK and BMP4 signaling pathways. Blood 116 (25), 5762-5772.

79. Demetz, G. et al. (2017) Overexpression of Insulin-Like Growth Factor-2 in Expanded Endothelial Progenitor Cells Improves Left Ventricular Function in Experimental Myocardial Infarction. J Vasc Res 54 (6), 321-328.

80. Quan, Z. et al. (2017) Thymosin β4 promotes the survival and angiogenesis of transplanted endothelial progenitor cells in the infarcted myocardium. Int J Mol Med 39 (6), 1347-1356.

81. Bai, Y.Y. et al. (2015) Synergistic Effects of Transplanted Endothelial Progenitor Cells and RWJ 67657 in Diabetic Ischemic Stroke Models. Stroke 46 (7), 1938-1946.

82. Aday, S. et al. (2017) Synthetic microparticles conjugated with VEGF165 improve the survival of endothelial progenitor cells via microRNA-17 inhibition. Nat Commun 8 (1), 747.

83. Soh, B.S. et al. (2016) Endothelin-1 supports clonal derivation and expansion of cardiovascular progenitors derived from human embryonic stem cells. Nat Commun 7, 10774.

84. Zangi, L. et al. (2013) Modified mRNA directs the fate of heart progenitor cells and induces vascular regeneration after myocardial infarction. Nat Biotechnol 31 (10), 898-907.

85. Vrijsen, K.R. et al. (2010) Cardiomyocyte progenitor cell-derived exosomes stimulate migration of endothelial cells. J Cell Mol Med 14 (5), 1064-1070.

86. Gallego-Perez, D. et al. (2017) Topical tissue nano-transfection mediates non-viral stroma reprogramming and rescue. Nat Nanotechnol 12 (10), 974-979.

87. Pashneh-Tala, S. et al. (2015) The Tissue-Engineered Vascular Graft-Past, Present, and Future. Tissue Eng Part B Rev, 68-100.

88. Fukunishi, T. et al. (2016) Tissue-Engineered Small Diameter Arterial Vascular Grafts from Cell-Free Nanofiber PCL/Chitosan Scaffolds in a Sheep Model. PLoS One 11 (7), e0158555.

89. Soletti, L. et al. (2010) A bilayered elastomeric scaffold for tissue engineering of small diameter vascular grafts. Acta Biomater 6 (1), 110-122.

90. Xu, S. et al. (2017) Preparation and characterization of small-diameter decellularized scaffolds for vascular tissue engineering in an animal model. Biomed Eng Online 16 (1), 55.

91. Elliott, M.B. and Gerecht, S. (2016) Three-dimensional culture of small-diameter vascular grafts. J Mater Chem B 4 (20), 3443-3453.

92. Krawiec, J.T. et al. (2016) In Vivo Functional Evaluation of Tissue-Engineered Vascular Grafts Fabricated Using Human Adipose-Derived Stem Cells from High Cardiovascular Risk Populations. Tissue Eng Part A 22 (9-10), 765-775.

93. Syedain, Z.H. et al. (2017) A completely biological "off-the-shelf" arteriovenous graft that recellularizes in baboons. Sci Transl Med 9 (414), eaan4209.

94. Bajpai, V.K. and Andreadis, S.T. (2012) Stem cell sources for vascular tissue engineering and regeneration. Tissue Eng Part B Rev 18 (5), 405-425.

95. Garreta, E. et al. (2017) Tissue engineering by decellularization and 3D bioprinting. Mater Today 20 (4), 166-178.

96. Faulk, D.M. et al. (2015) Decellularization and cell seeding of whole liver biologic scaffolds composed of extracellular matrix. J Clin Exp Hepatol 5 (1), 69-80.

97. Ott, H.C. et al. (2008) Perfusion-decellularized matrix: using nature's platform to engineer a bioartificial heart. Nat Med 14 (2), 213-221.

98. Ren, X. et al. (2015) Engineering pulmonary vasculature in decellularized rat and human lungs. Nat Biotechnol 33 (10), 1097-1102.

99. Gao, L.P. et al. (2017) Use of human aortic extracellular matrix as a scaffold for construction of a patient-specific tissue engineered vascular patch. Biomed Mater 12 (6), 065006.

100. Mertsching, H. et al. (2005) Engineering of a vascularized scaffold for artificial tissue and organ generation. Biomaterials 26 (33), 6610-6617.

101. Schultheiss, D. et al. (2005) Biological vascularized matrix for bladder tissue engineering: matrix preparation, reseeding technique and short-term implantation in a porcine model. J Urol 173 (1), 276-280.

102. Mao, S.A. et al. (2017) Sustained In Vivo Perfusion of a Re-Endothelialized Tissue Engineered Porcine Liver. Int J Transplant Res Medi 3 (1), 1-9.

103. Hospodiuk, M. et al. (2017) The bioink: A comprehensive review on bioprintable materials. Biotechnol Adv 35 (2), 217-239.

104. Zhu, W. et al. (2017) Direct 3D bioprinting of prevascularized tissue constructs with complex microarchitecture. Biomaterials 124, 106-115.

105. Mirabella, T. et al. (2017) 3D-printed vascular networks direct therapeutic angiogenesis in ischaemia. Nat Biomed Eng 1 (6), 0083.

106. Braghirolli, D.I. et al. (2017) Electrospun scaffolds functionalized with heparin and vascular endothelial growth factor increase the proliferation of endothelial progenitor cells. Biomed Mater 12 (2), 025003.

107. Duan, B. et al. (2013) 3D bioprinting of heterogeneous aortic valve conduits with alginate/gelatin hydrogels. J Biomed Mater Res A 101 (5), 1255-1264.

108. Melchiorri, A.J. et al. (2015) Contrasting biofunctionalization strategies for the enhanced endothelialization of biodegradable vascular grafts. Biomacromolecules 16 (2), 437-446.

CHAPTER 3

HUMAN PLURIPOTENT STEM CELL-DERIVED MULTIPOTENT VASCULAR PROGENITORS: UTILITY IN TISSUE ENGINEERING AND REPAIR[2]

[2] Colunga, T., Hayworth, M., Kreß, S., Reynolds, D.M., Chen, L., Nazor, K., Kulik, M., Menendez, L., Baur, J., Singh, A.M., Loring, J.F., Metzger, M., Dalton, S. 2018. Submitted to *Nature Medicine*, 04/21/18.

ABSTRACT

In this report we describe a novel, human pluripotent stem cell-derived vascular progenitor (MesoT) cell of the mesothelium lineage. MesoT cells are multipotent and generate smooth muscle cells, endothelial cells and pericytes and self-assemble into vessel-like networks *in vitro*. MesoT cells transplanted into mechanically damaged neonatal mouse heart migrate into the injured tissue and contribute to nascent coronary vessels in the repair zone. When seeded onto decellularized vascular scaffolds, MesoT cells differentiate into the major vascular lineages and self-assemble into vasculature capable of supporting peripheral blood flow following transplantation. These findings demonstrate the potential utility of MesoT cells in tissue repair and vascular engineering applications.

INTRODUCTION

Coelomic organs including the heart, spleen, lungs, liver and gut are lined on their outer surface by a thin layer of cells with epithelial characteristics known as visceral mesothelium[1]. During early development, mesothelium is highly dynamic and critical for growth and maintenance of the underlying tissue. Following the formation of the mesothelial layer, a subpopulation of these cells undergoes an epithelial to mesenchymal transition (EMT) and invade the underlying tissue. Here, they transition through a mesenchymal progenitor intermediate and in response to local signals they differentiate into vascular lineages, which contribute to a nascent vascular network[2-9]. Mesothelium-derived progenitor cells with mesenchymal characteristics have been described in the heart[2,3,10], gut, lungs and liver[3] and contribute to vascularization of these organs during

embryonic development and possibly during tissue regeneration[11,12]. Numerous reports have also highlighted the broad potential of mesothelium and mesothelium-derived cells in tissue repair[1,13-15]. For example, the epicardium and its derivatives have been implicated in regenerative responses following myocardial infarction[11,13,16] and mechanical injury[17].

In this report, we describe the generation of a multipotent, vascular progenitor cell of the mesothelium lineage (MesoT) from human pluripotent stem cells (hPSCs). In addition to being a potential source of cells for revascularization of damaged tissue, MesoT cells are shown to have potential utility in tissue engineering contexts. This is of significance because current tissue engineering approaches for generating transplantable blood vessels of small-medium diameter (<5mm) have significant limitations. The availability of hPSC-derived, multipotent vascular progenitors opens up new opportunities for the advancement of tissue engineering and regenerative medicine.

RESULTS

A hPSC-derived cell of the mesothelium lineage with vascular characteristics

During embryonic development, cardiovascular lineages are generated from a transient splanchnic mesoderm (SplM) progenitor population. Equivalent cells can be generated at high efficiency from hPSCs in chemically defined media (CDM) containing BMP4 (**Fig. 1a** and **Supplementary Fig. 1a-d**). These cells have epithelial characteristics ($ZO1^+$, αSMA^-, VIM^-) (**Fig. 1b**), express transcription factors that are characteristic of SplM including ISL1, NKX2.5 and GATA4 (**Fig. 1b,c** and **Supplementary Fig. 1a,b**) and show decreased levels of pluripotency markers NANOG, OCT4 and SOX2

(**Supplementary Fig. 1c,d**). While smooth muscle cells (SMCs)[18-20] and endothelial cells (ECs)[20,21] have been directly generated from hPSC-derived mesoderm, a multipotent progenitor equivalent to a tissue-derived vascular precursor has not been reported. The availability of a progenitor cell with these characteristics could have utility in revascularization of damaged tissue or potentially in vascular engineering.

While attempting to identify novel derivatives of hPSC-derived mesoderm, we found that treatment of SplM with all-*trans* retinoic acid (RA) promoted a uniform morphological transformation, representative of a new cell type being formed (**Fig. 1b**). RA treatment downregulated SplM markers (ISL1, NKX2.5)(**Fig. 1b,c**) and promoted an EMT, as shown by loss of ZO1 and increased vimentin and αSMA expression (**Fig. 1b**). The RNA-seq signature of RA-treated cells was then compared to that of human and mouse tissues to identify the lineage of these cells (**Fig. 1a**). Hierarchical clustering analysis of RNA-seq data showed that RA-treated SplM clustered with primary human epicardium and mouse mesothelium isolated from heart, liver, lung and gut (**Fig. 1d**), suggesting that it belongs to the mesothelium lineage (MesoT). Although MesoTs exhibit characteristics of embryonic mesothelium at the molecular level such as the expression of transcription factors WT1, TBX18 and TCF21 (**Fig. 1b,c and Supplementary Fig. 1e-g**) they also have mesenchymal characteristics (αSMA^+, VIM^+, $ZO1^-$) (**Fig. 1b**). This contrasts with the typical epithelial characteristics of mesothelium but is reminiscent of mesothelium-derived mesenchymal cells that invade the underlying tissue during organogenesis[4,6,8,9].

To determine whether MesoTs are descendants of mesothelium, we repeated differentiation of SplM in CDM supplemented with BMP4 and RA but in the absence of

factors known to promote EMT (Activin A and Fgf2)(**Supplementary Fig. 2a**). This set of conditions generated epithelial cells that expressed mesothelium markers (**Supplementary Fig. 2b,c**), which will be designated as "mesothelium-like cells" (MLCs). Once Activin A and Fgf2 signaling was restored, MLCs transitioned through an EMT and towards a phenotype reminiscent of MesoTs at the molecular and cellular level (**Supplementary Fig. 2c**). These results are consistent with the development of hPSC-derived SplM along the mesothelium lineage[22,23]; first through an epithelial state (MLCs) followed by a migratory state (MesoTs).

Since mesothelium-derived cells have been implicated in vascular development during embryogenesis[2,3], we sought to obtain corroborative evidence that MesoT cells have vascular potential by characterizing their epigenetic signature. We identified a MesoT-specific CpG methylation signature that is non-overlapping with corresponding signatures for SplM, hPSC-derived cardiomyocytes and hPSCs. A cohort of 1846 methylated CpGs were identified that fulfilled this condition (**Supplementary Fig. 3a**). This signature was used to screen an expanded panel of DNA methylation datasets including 30 primary human tissues and primary cell samples. This approach showed that primary SMCs, primary ECs and umbilical cord cells have a similar methylation signature to MesoT cells (**Fig. 2a**). This indicates that MesoT cells have epigenetic marks consistent with being part of the vascular lineage.

If MesoTs are precursors for either SMCs or ECs it would be anticipated that enhancers required for specification of these vascular lineages would be in a H3K4me1^{high} H3K27ac^{low} 'primed' state[24,25] in MesoTs (**Fig. 2b).** To address this, the epigenetic state of active enhancers (H3K27ac^{high}) linked to transcriptionally upregulated

gene sets in primary SMCs and ECs were analyzed in MesoTs by ChIP-seq (**Fig. 2c and Supplementary Table 1**). These results show that active enhancers linked to vascular transcriptional programs are in a primed state in MesoT cells, in contrast to the active state in SMCs and ECs (**Fig. 2d**). Gene ontology analysis shows that epigenetically-primed ($H3K4me1^{high}$ $H3K27ac^{low}$) enhancers in MesoTs are linked to genes that are significantly enriched for functions in vascular development and activity (**Supplementary Fig. 3b,c**). Since epigenetic analysis pointed towards MesoTs being part of the vascular lineage, a more focused RNA-seq analysis was also performed. Principal component analysis (PCA) of RNA-seq data shows that MesoTs cluster with SMCs, ECs, primary and hESC-derived epicardium but segregate away from hESCs, ectoderm and endoderm lineages (**Fig. 2e**). Together, these results are consistent with the hypothesis that MesoTs are of the vascular lineage and are precursors for SMCs and ECs.

MesoTs are multipotent vascular progenitor cells

With global transcript and epigenetic analysis suggesting MesoT cells as vascular progenitors of mesothelial origin, we next sought to evaluate the differentiation potential of these cells *in vitro*. MesoT cells were treated with PDGFβ or with a combination of VEGF and the ALK4 inhibitor SB431542, conditions known to promote the differentiation of mesoderm cells to smooth muscle cell[3,26] and endothelial cell[21] identities, respectively. PDGFβ treatment of MesoTs yielded cultures in which ~85% cells expressed the SMC markers calponin, alpha smooth muscle actin (αSMA) and myosin heavy chain 11 (MYH11)(**Fig. 3a,b**). The amplification in cell number as hPSCs transitioned to SMCs through a MesoT progenitor state is approximately 30-fold

(**Supplementary Fig. 4a**). Although MesoTs are αSMA^+ they are distinguished from SMCs based on their differential expression of markers such as calponin, MYH11 and WT1 (**Fig. 3a and Supplementary Fig. 4b,c**). Treatment with the acetylcholine receptor agonist carbachol and the membrane depolarizing agent KCl both triggered cell contraction within 30 minutes (**Fig. 3c,d**), responses expected of SMCs. These observations indicate that MesoTs are capable of efficiently generating SMCs when treated with PDGFβ.

Treatment of MesoTs with VEGF and SB431542 uniformly increased the expression of endothelial markers von Willebrand factor (vWF), CD31 and VE-cadherin (**Fig. 3e,f**). Endothelial cell markers such as vWF and CD31 are not expressed in MesoTs or in SMCs (**Supplementary Fig. 4b,d,e**). Functional characterization of VEGF/SB-treated cells was first evaluated using *trans*-endothelial electrical resistance (TEER) assays after plating cells on a transwell system coated with a collagen IV-fibronectin matrix. Here, TEER of MesoTs treated with SB/VEGF increased over 28 days and was comparable or greater than that observed for primary human endothelial cells (**Fig. 3g**). FITC-dextran diffusion was assessed across cell monolayers treated with VEGF/SB. It was expected that if VEGF/SB treated MesoTs generated selectively permeable endothelial cells they would resist diffusion of FITC-dextran (40 kDa) across the monolayer. As expected, primary endothelial cell monolayers allowed only low levels of label to diffuse through the cellular layer. The extent of FITC-dextran retention was even greater in VEGF alone or VEGF/SB treated MesoT cells (**Fig. 3h**), consistent with formation of a tight epithelial barrier. When cultured on a collagen IV-fibronectin-coated transwell insert (**Fig. 3i**), ECs generated from MesoTs formed a layer of cells expressing

the tight junction protein ZO1 (**Fig. 3j**). When examined by transmission electron microscopy, cells exhibited typical endothelial architecture with tight junctions (**Fig. 3k**). Together, these data show that functional endothelial cells can be generated from MesoT progenitors at high efficiency. The overall cell amplification as hPSCs differentiate to ECs through a MesoT intermediate is ~50-fold (**Supplementary Fig. 4a**). The ~30-fold amplification to SMCs and 50-fold amplification to ECs indicates that differentiation of MesoT progenitor cells results in significant amplification of vascular lineages.

To obtain evidence that MesoT cells are multipotent vascular progenitors it was necessary to establish culture conditions in which MesoT cells could be amplified for approximately 15-20 days to allow for clonal amplification. CDM did not support maintenance and proliferation of MesoT cells over this timeframe but supplementation with fetal bovine serum supported maintenance for up to 9 passages. During this period, MesoTs retained their proliferative capacity (**Fig. 4a**), cell cycle properties (**Fig. 4b-d**) and global transcriptome profile (**Fig. 2e**). By interrogating RNA-seq data we identified several cell surface markers expressed on the surface of MesoTs that were absent on SplM, making these markers potentially useful for cell purification and single cell analysis. To confirm the utility of these markers, which include CD44, CD73, and CD105, triple $CD44^+/CD73^+/CD105^+$ MesoT cells were isolated, sorted into 96-well dishes and, following amplification, differentiated under smooth muscle (+PDGFβ) and endothelial cell (+VEGF) conditions (**Fig. 4e,f**). All 14 amplified clones showed SMC ($MYH11^+$) and EC (vWF^+) differentiation capacity under the respective conditions, although individual clones showed different potencies (**Fig. 4g**). We conclude that

MesoTs are multipotent vascular progenitor cells, confirming predictions made from the earlier molecular analysis (**Figs. 2,3**).

We reasoned that multipotent MesoT cells could give rise to mixed populations of SMCs and ECs. By this rationale, we determined that CDM -Activin A supplemented with VEGF was sufficient to support the differentiation of MesoTs into mixtures of SMCs and ECs (**Fig. 4h**). Under these conditions, both cell types were generated in approximately equal proportions. When cultured under these conditions for >12 days, mixed populations of SMCs and ECs self-assembled into vessel-like networks (**Fig. 4i**). The composition and organization of such 'vessels' was evaluated by immunofluorescence (IF) and were shown to be composed of vWF^+ ECs and αSMA^+ SMC/pericyte-like cells (**Fig. 4j**). vWF^+ cells formed the core of these structures while αSMA^+ cells were generally located around the periphery. This is an interesting observation because it establishes conditions in which a single progenitor cell (MesoTs) can give rise to SMCs and ECs under the same culture conditions that can self-assemble into a simple vessel structure.

MesoTs contribute to *neo*-vascularization during tissue repair

To investigate the vascular potential of MesoT cells in a tissue injury context we used a murine neonatal heart repair model[17]. Following resection of the ventricular apex, the neonatal mouse heart undergoes repair including partial muscle regeneration and *neo*-vascularization with variable fibrosis[17,27,28]. Work in zebrafish suggests that mesothelium-derived cells may be part of such a response by contributing to peri-vascular cells[12,29]. To determine whether MesoTs have capacity for vascular repair, they were injected into the

pericardial space of P0.5 mouse pups, adjacent to the resected tissue (**Fig. 5a,b and Supplemental Fig. 5a,b**). 30 days after transplantation mice were sacrificed and cardiac tissue was analyzed by immunohistochemistry on cryosections. Mice receiving saline alone (n=11) or MesoT cells (n=13) revascularized the injured heart. In each heart receiving MesoTs, a major contribution to coronary vessels in repair zones was made by $hGolgi^+$ $CD31^+$ human cells (**Fig. 5c**). These vessels were connected to the host vasculature as indicated by the presence of erythrocytes (**Supplementary Fig. 5c**). Further analysis showed that $hGolgi^+$ $CD31^+$ endothelial cells and hGolgi αSMA^+ SMC/pericyte-like cells made significant contributions to the *neo*-vasculature in repair zones (**Fig. 5d**). These results show that MesoT progenitor cells can differentiate and assemble into functional vessels in this tissue injury model and suggests that they may be useful in a broader range of regenerative approaches.

Vascularization of biological scaffolds by MesoTs: *in vitro* and *in vivo* function

The cell culture and *in vivo* experiments presented suggest that MesoT cells may be a viable alternative to existing approaches for the re-cellularization of vascular scaffolds used for tissue engineering. To investigate this possibility we used explanted, decellularized rat jejunal segments (**Fig. 6a**) as a biological scaffold on which to seed MesoT cells in a bioreactor (**Supplementary Fig. 6a**). In this model, the rat vasculature remains intact and can be perfused using the afferent artery and efferent vein (**Fig. 6b,c**). Following the introduction of MesoT cells through the lumen of the vascular bed, constructs were perfused with medium supporting differentiation to SMCs and ECs (**Fig. 4h-j**). Perfusion was pulsatile and increased gradually to a physiological pressure of 80-

120 mmHg to promote vessel maturation. Constructs were then perfused with 3-(4,5-dimethylthiazol-2-yl)-2,5-diphenyltetrazolium bromide (MTT), a substrate used to evaluate the assembly of metabolically active cells in the vascular network (**Fig. 6d**). This shows that viable cells broadly lined the jejunal scaffold and that these cells were of human origin (**Fig. 6e**). No MTT staining was observed in constructs that were not recellularized (**Supplementary Fig. 6b**). Analysis of vessels by IF on cryo-sections showed that capillaries were lined with human $CD31^+$ cells and that medium (~100-150 μm) and larger (>150 μm) vessels were lined with $CD31^+$ cells and αSMA^+ cells. The organization of these cells was as expected, with CD31+ endothelial cells forming a contiguous layer on the lumenal surface and αSMA^+ SMCs forming an adjacent layer on the ablumenal side (**Fig. 6f-h**). The perfusion of decellularized vascular beds with MesoT cells supports their differentiation and self-assembly into vascular structures; this is reminiscent of their behavior in two-dimensional culture (**Fig. 4h-j**).

To evaluate the barrier function of MesoT-derived cells in the vascular structures, cellularized constructs were perfused with FITC-dextran and monitored by time lapse imaging. We observed that MesoT-derived vessels retained FITC-dextran (**Fig. 6i** and **Supplementary Video 1**) in contrast to constructs that were sparsely-seeded where rapid diffusion and leakage was observed (**Supplementary Fig. 6c**). Scaffolds without cells are not shown because label leaks immediately at the site of infusion and can't be visualized. Endothelial cell function was verified by demonstrating the uptake of acetylated low-density lipoprotein (**Fig. 6i**). To determine the extent to which MesoT-derived endothelium lined the vascular tree, we stained perfused constructs with human-specific anti-CD31 antibody. Light sheet microscopy (LSM) showed widespread incorporation of

these cells into the vasculature (**Fig. 6j**, **Supplementary Fig. 6d,e and Supplementary Video 2**), as expected from our analysis of the frozen sections (**Fig. 6f-h**). LSM also showed incorporation of $NG2^+$ pericyte-like cells into vascular networks (**Supplementary Fig. 6f**). This indicates that MesoT cells can contribute to three vascular lineages.

To investigate the functionality of MesoT-populated vascular constructs under physiological conditions, recellularized jejunal scaffolds were connected to the rat circulation by anastomosis (**Fig. 6k**) for 3 days. Analysis of anastomosed constructs showed that vessels retained gross morphologic integrity with no indication of blood leakage or occlusion (**Fig. 6l, Supplementary Fig. 6g)**. Further analysis of these vessels by IF following cryo-sectioning showed maintenance of capillaries and larger vessels, in composition and architecture, after anastomosis (**Fig. 6m-o**). These observations show that MesoTs can populate biological scaffolds with cells that assemble into vessels which withstand physiological pressures and conditions, at least over short periods of time.

DISCUSSION

In this report, we have characterized a mesenchymal cell of the mesothelium lineage that has multipotent vascular potential. Embryonic mesothelial layers of different coelomic organs have similar molecular and cellular characteristics[3,30] (**Fig. 1d**) but because the developmental pathway for each has not been clearly defined, it is not possible to unequivocally assign mesothelium-like cells (MLCs) and MesoTs to mesothelium from a specific anatomical location (e.g. the heart). In the absence of specific information to address this issue, we have designated MLCs and MesoT cells as

being of 'mesothelial origin'. Several reports have described the generation of 'epicardium' from hPSCs[31,32] and although these cells are potentially generated along similar developmental pathways as MesoT cells, they differ in several key respects. First, 'epicardium' cells are epithelial and develop through a 'pro-epicardium' stage[32]. Second, hPSC-derived 'epicardium' has a propensity for SMC and fibroblast differentiation, with no multipotency or endothelial potential reported. It has been proposed that the pro-epicardium and epicardium are heterogeneous in cell composition[33,34], making different contributions to the coronary vasculature. It is possible that hPSC-derived 'epicardium' and the mesothelium described here, are representative of different mesothelial subtypes. Alternatively, they could represent completely different organ-specific mesothelium lineages associated with different anatomical locations *in vivo*. We hypothesize from a developmental standpoint, that MLCs represent mesothelium and that MesoTs are their vasculogenic mesenchymal descendants[3,10,35].

Several reports have described mesenchymal progenitor descendants of the epicardial lineage[3,10,35,36]. For example, epicardium-derived cells (EPDCs) have a propensity for smooth muscle cell and fibroblast/stromal cell contribution but not towards an endothelial identity[36]. Lineage-marked descendants of mesothelium from multiple organs have been isolated and shown to have a similar potency to EPDCs[3]. While there is some debate about the degree to which EPDCs contribute to the endothelium of the coronary vasculature[37], several studies indicate some contribution of the epicardium lineage to arterial vessels with the remainder coming from other sources[33,38-41]. Whether this endothelial contribution comes from EPDCs or another epicardial subtype is not known. The MesoT cells described in this report are likely to be one subpopulation of

resident mesothelium-derived progenitor cells that contribute to the vasculature of coelomic organs such as the heart. We are not aware of any other reported cell type from the mesothelium lineage that has the multipotent, vascular progenitor characteristics of that described here for MesoT cells.

hPSC- and tissue-derived vascular cell types, including smooth muscle cells and endothelial cells, have been used for the development of cell therapeutics and tissue engineering[42,43], providing proof of concept for this strategy. However, barriers to using these cell types in vascular repair scenarios exist and need to be considered if PSC-derived vascular cells are to become clinically viable. For example, fully differentiated SMCs and ECs have not yet been shown to efficiently incorporate into new vasculature in a tissue repair model following transplantation. This could be related to limitations of mature cells to integrate into remodeling tissue or an inability to assemble into *neo*-vessels in a repair environment. In tissue engineering, combinations of SMCs, ECs and MSCs are frequently used to seed vascular scaffolds, but this process is complicated and the long-term efficacy of such constructs are unclear[43-46]. Our results suggest that vascular progenitor cells may be a solution to the problems associated with using mature vascular cell types. In support of this idea, circulating endothelial progenitor cells (EPCs) first identified *in vivo*[47,48], but also recently derived from hPSCs, show functional efficacy by contributing to new vasculature in a diabetic retinopathy model[49]. Although EPCs have promising clinical utility, their potency is restricted to the endothelial lineage. These limitations do not apply to MesoT cells because of their vasculogenic, multipotent properties. Moreover, MesoT cells can differentiate into vascular lineages that self-

assemble into complex, multilayered vascular structures. These properties open up many opportunities for the use of MesoTs in tissue repair and tissue engineering.

Acknowledgements

Work in SD laboratory was supported by NIH grants P01 HL089471 and P01 GM75334; JFL and KN were supported by the California Institute for Regenerative Medicine (RT1-01108, RT3-07655, TR1-01250, TR3-05603, and CL1-00502), and NIH (R01NS092042); SK and MM were supported by the Bavarian Research Foundation (AZ-1044-12) and Bavarian FIT Program. We thank Andy Wessels for many useful discussions and Charles Murry for hPSC-derived cardiomyocyte samples for genomic analysis. We thank Julie Nelson of the UGA CTEGD Cytometry Shared Resources Laboratory for continued help with flow cytometry and cell sorting.

TC, MH, DMR and KN contributed to Fig. 1. TC, LC and AMS provided materials while LC and KN conducted bioinformatics analysis for Fig. 2. TC and MH contributed to Fig. 3a-f and SK generated Fig. 3g-k. TC and LC generated Fig. 4a-h and MH generated Fig. 4i,j. TC and MH obtained and generated data for Fig. 5. Fig. 6 was developed and generated by MM, SK and JB. TC, MH and DMR generated Suppl. Fig. 1. LC supplied data for Suppl. Fig. 2. LC and KN conducted analysis for Suppl. Fig. 3. TC and MH equally contributed to Suppl. Fig. 4. MH supplied images for Suppl. Fig. 5. MM, SK and JB contributed data for Suppl. Fig. 6 and Suppl. Videos 1 and 2.

Figure 3.1 | hPSC-derived MesoT displays molecular characteristics of primary mesothelium.

a) Sources of cells used for RNA-seq analysis. hPSC-derived MesoT cells and tdTomato+ mesothelium isolated from mouse embryonic gut, liver, heart and lungs (E15.5) were compared to RNA-seq data in the public domain. **b)** Addition of BMP4 and retinoic acid (RA) to SplM ($ISL1^+$, $NKX2.5^+$, $ZO1^+$) efficiently generates MesoT ($WT1^+$, αSMA^+, VIM^+) with a mesenchymal phenotype. Scale bars, 50 μm. **c)** qRT-PCR data showing fold-change of transcript levels for markers of SplM (*ISL1*, *NKX2.5* and *GATA4*) and MesoT (*WT1*, *TBX18* and *TCF21*) following directed differentiation of hESCs (WA09). TaqMan assays for each transcript were performed in technical triplicate and fold-change shown relative to untreated hESCs (WA09) after normalization with 18S RNA. Error bars +/- standard deviation. **d)** Left: hierarchical clustering (Euclidean distance, complete linkage) of all human (black box) and mouse (red box) RNA-seq samples according to mouse and human orthologs. Data from both species were log transformed and scaled to mean=0 and standard deviation=1 prior to clustering. Right: zoomed-in section of the highlighted portion of the array tree dendrogram (left panel) showing that hPSC-derived MesoT are closely related to human (h) and adult (a) epicardium; mouse (m) and fetal (f) mesothelium. Replicate numbers from independent experiments are indicated.

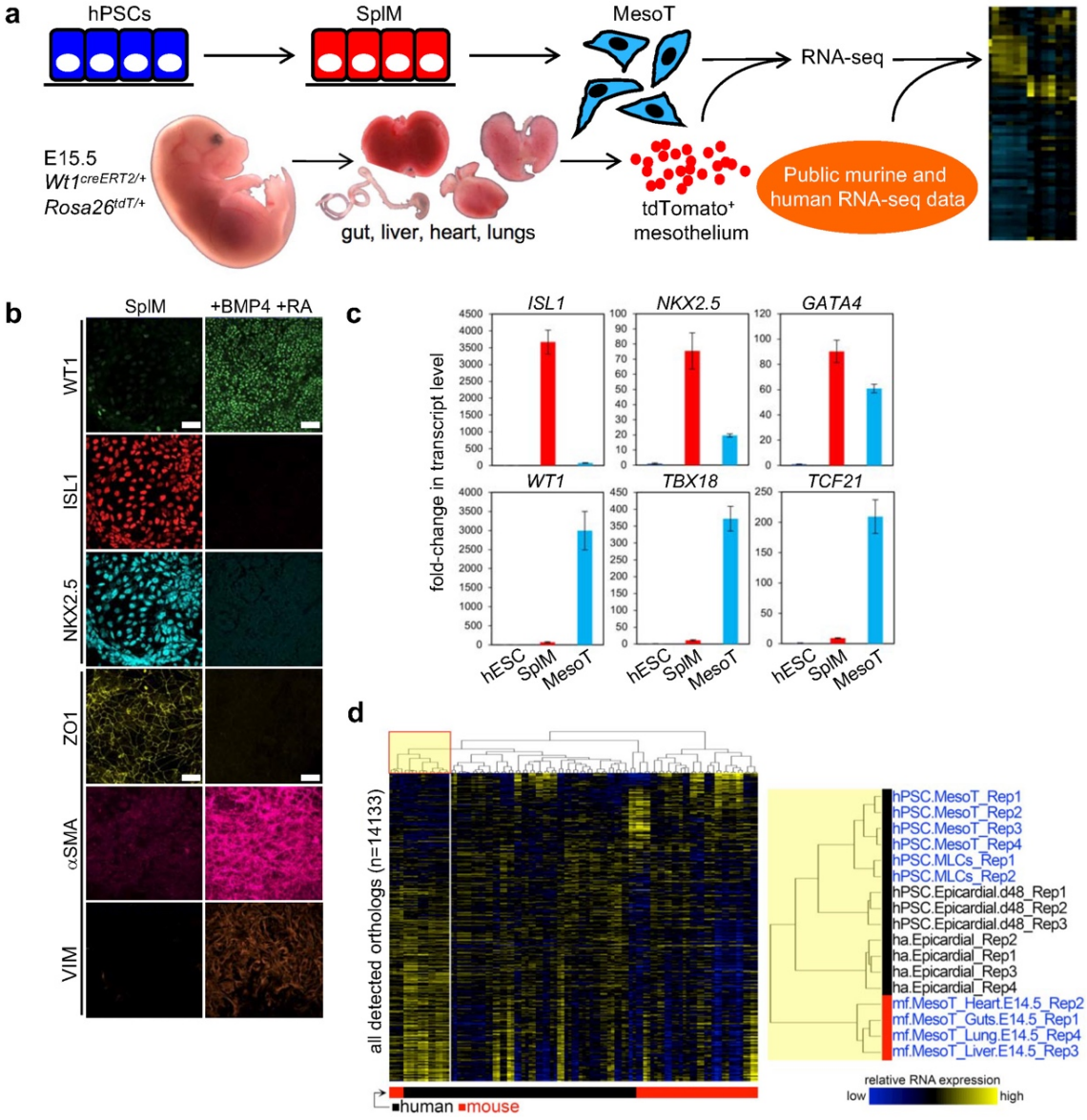
a
hPSCs
SplM
MesoT
RNA-seq
E15.5
Wt1creERT2/+
Rosa26tdT/+
gut, liver, heart, lungs
tdTomato+
mesothelium
Public murine and
human RNA-seq data
b
SplM
+BMP4 +RA
WT1
ISL1
NKX2.5
ZO1
αSMA
VIM
c
ISL1
NKX2.5
GATA4
WT1
TBX18
TCF21
fold-change in transcript level
hESC
SplM
MesoT
d
all detected orthologs (n=141133)
human
mouse
hPSC.MesoT_Rep1
hPSC.MesoT_Rep2
hPSC.MesoT_Rep3
hPSC.MesoT_Rep4
hPSC.MLCs_Rep1
hPSC.MLCs_Rep2
hPSC.Epicardial.d48_Rep1
hPSC.Epicardial.d48_Rep2
hPSC.Epicardial.d48_Rep3
ha.Epicardial_Rep2
ha.Epicardial_Rep1
ha.Epicardial_Rep3
ha.Epicardial_Rep4
mf.MesoT_Heart.E14.5_Rep2
mf.MesoT_Guts.E14.5_Rep1
mf.MesoT_Lung.E14.5_Rep4
mf.MesoT_Liver.E14.5_Rep3
relative RNA expression
low
high

Figure 3.2 | Epigenetic and transcript profiles of MesoT are similar to vascular cell types.

a) Hierarchical clustering (Euclidean distance, complete linkage) of human tissue and hESC-derived samples according to Beta values for the 1846 cytosines comprising module 9 of the DNA methylation profile. Array tree dendrograms and the distribution of Beta values for these cytosines are presented in heatmap form (top) and as box and whisker plots (bottom). **b)** Cartoon depicting the epigenetic landscape at primed and activated enhancers as MesoT cells transition to a vascular fate. Top portion depicts vascular genes 'primed' in MesoT with the presence of K4me1 on histone H3 at enhancer sites. Bottom portion depicts the primed enhancers for vascular genes being activated by addition of K27ac as they differentiate to smooth muscle cells (SMCs) or endothelial cells (EC). **c)** Enhancer and gene ontology discovery pipeline for data in **(d, Supplementary Fig. 3b,c)**. **d)** Heatmaps of H3K4me1 (red) and H3K27ac (blue) ChIP-seq data for enhancers linked to up-regulated genes in primary smooth muscle and endothelial cells, compared to MesoTs. **e)** Principal component analysis of the top 20% of up-regulated genes in hESC-derived mesoderm cells and primary fetal and adult (epicardium) samples. MesoT (CDM) and MesoT (FBS) (self-renewing) cells cluster tightly with vascular cell types (ECs and SMCs) and mesothelium.

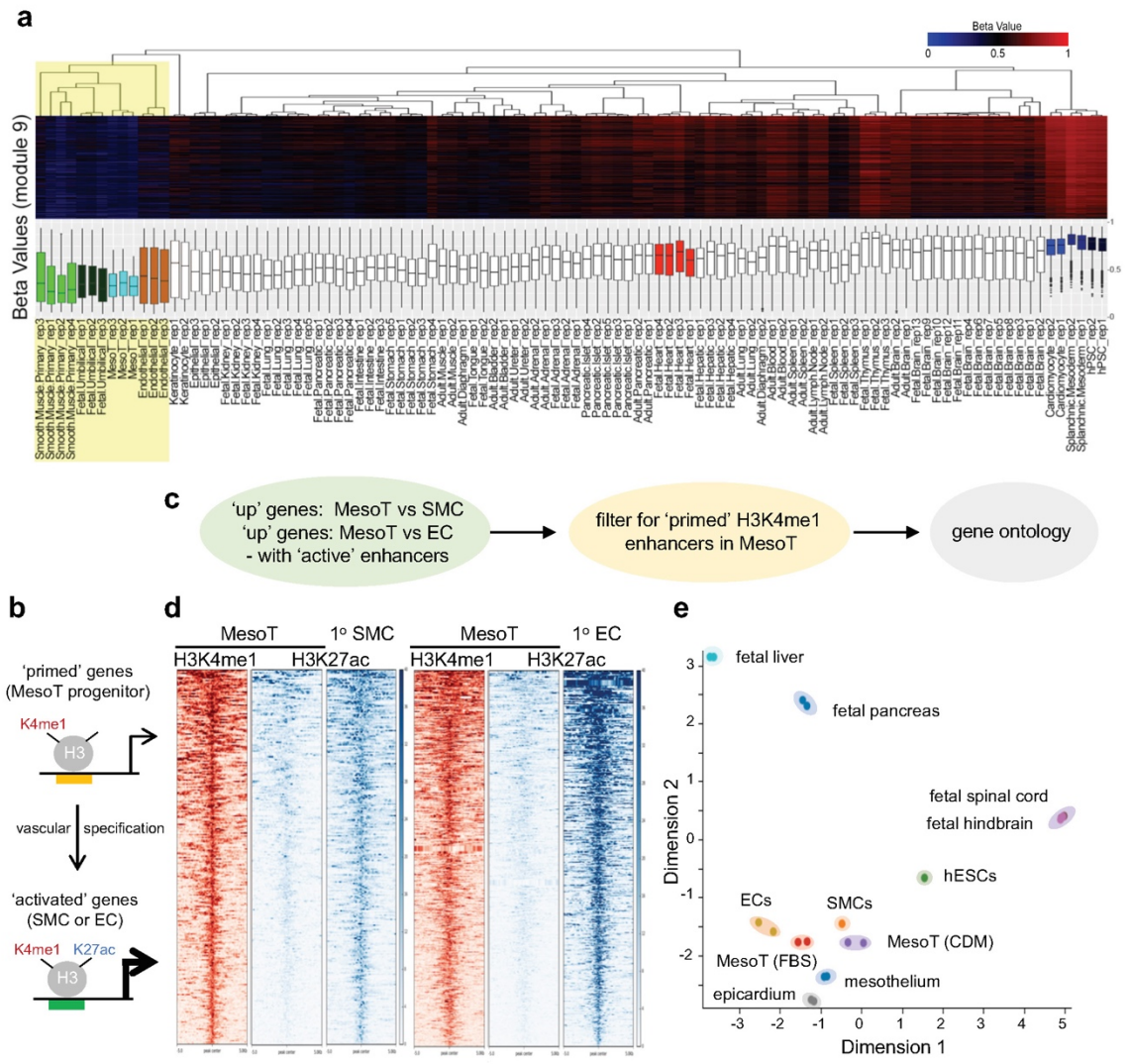
a
Beta Value
0
0.5
1
Beta Values (module 9)
b
'primed' genes
(MesoT progenitor)
K4me1
H3
vascular specification
'activated' genes
(SMC or EC)
K4me1 K27ac
H3
c
'up' genes: MesoT vs SMC
'up' genes: MesoT vs EC
- with 'active' enhancers
filter for 'primed' H3K4me1
enhancers in MesoT
gene ontology
d
MesoT
1° SMC
MesoT
1° EC
H3K4me1
H3K27ac
H3K4me1
H3K27ac
e
fetal liver
fetal pancreas
fetal spinal cord
fetal hindbrain
hESCs
ECs
SMCs
MesoT (CDM)
MesoT (FBS)
mesothelium
epicardium
Dimension 1
Dimension 2

Figure 3.3 | MesoT efficiently differentiate to smooth muscle and endothelial cells. **a)** MesoT cells treated with PDGFβ (50 ng/ml) in CDM -Activin A for 12 days were probed with antibodies for alpha smooth muscle actin (αSMA), calponin and myosin heavy chain 11 (MYH11). Scale bars, 100 μm (left) and 50 μm (right). **b)** MesoTs grown in CDM (-A) supplemented with PDGFβ or VEGF-A_{165} and SB431542. **c)** DiO labeled SMCs as shown in **(a)** were treated with 100 μM carbachol or 50 mM KCl. **d)** SMC surface area was measured after treatment. Contraction is shown as the % change in cell surface area for individual cells. Each treatment group was compared to corresponding control time point to determine statistical significance. n=20, error bars +/- SEM, **** p-value<0.0001. **e)** MesoT cells treated with CDM (-A), VEGF-A_{165} and SB431542 for 12 days were fixed and probed with antibodies for CD31, vWF and DAPI or, **(f)** characterized by flow cytometry with VE-cadherin (blue) or isotype control (red). Scale bar, 50 μm. **g)** *Trans*-endothelial electrical resistance (TEER) was measured after culturing MesoT cells in CDM (-A) supplemented with VEGF-A_{165} alone (+VEGF) or with SB431542 (+VEGF +SB) after 14, 21 and 28 days and compared against primary dermal microvascular endothelium (1º ECs). n=3, error bars +/- SEM, ** p-value=0.0027. **h)** Barrier integrity was tested by measuring FITC-dextran (40 kDa) perfusion from the apical to basolateral side. Control represents the absence of cells. No statistical significance was determined when comparing cells to 1º ECs. Error bars +/- SEM. **i)** Schematic of the bioreactor culture system used in **(g)** and **(h)**. **j)** Immunofluorescence of cell monolayer as in **(i)** showing expression of tight junction marker ZO1 (top) and H&E staining (bottom). **k)** Transmission electron microscopy

image of MesoT-derived endothelium. Red arrows depict tight cell junctions. Inset (top) is depicted on bottom. Scale bars, 500 nm and 200 nm, respectively.

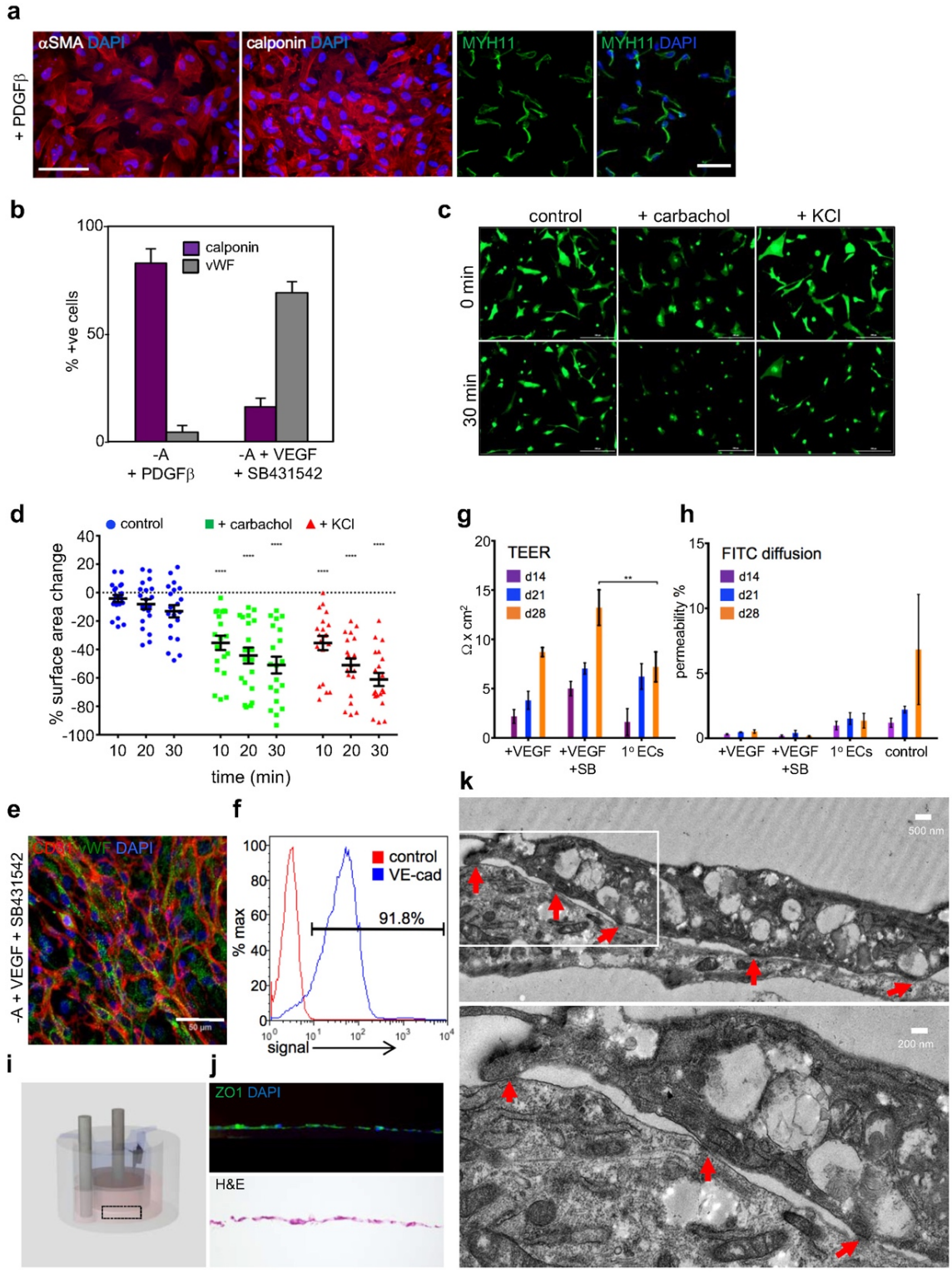
a
αSMA DAPI
calponin DAPI
MYH11
MYH11 DAPI
+ PDGFβ
b
% +ve cells
calponin
vWF
-A
+ PDGFβ
-A + VEGF
+ SB431542
c
control
+ carbachol
+ KCl
0 min
30 min
d
control
+ carbachol
+ KCl
% surface area change
time (min)
g
TEER
d14
d21
d28
Ω x cm²
+VEGF
+VEGF +SB
1° ECs
h
FITC diffusion
permeability %
control
e
-A + VEGF + SB431542
f
control
VE-cad
91.8%
% max
signal
i
j
ZO1 DAPI
H&E
k
500 nm
200 nm

Figure 3.4 | MesoTs are multipotent vascular progenitor cells.

a) Population doubling of MesoT (FBS) cells. Time=0 is when cells are first passed into serum containing media. Simple linear regression analysis (blue dashes) applied to data shows a tightly fitted regression line with a coefficient of determination (R^2) = 0.9774 and slope of 0.8282+/-0.0563. Experiment n=3 performed in technical triplicate. Error bars +/- SEM. **b)** Cell cycle analysis of self-renewing MesoT (FBS) cells at passage 4 and 9 using Life Technologies Click-iT® Plus EdU Alexa Fluor® flow cytometry assay kit. n=4 for p4 & n=3 for p9, all in technical triplicate. Error bars +/- SEM. **c-d)** Representative two-dimensional flow plots for each passage showing gating strategy to determine % of cells in each cell cycle phase for **(b)**. **e)** Clonal assay strategy to determine multipotency of self-renewing MesoT (FBS). **f)** FACS gating strategy to obtain single cells for clonal analysis. Triple positive single cells ($CD44^+/CD73^+/CD105^+$) were sorted onto a 96 well plate for amplification and downstream lineage analysis. **g)** After amplification, 14 individual clones were selected for downstream lineage analysis. MesoT (FBS) cells were treated with 2% FBS +VEGF or +PDGFβ for endothelial or smooth muscle cell differentiation, respectively. Cells were fixed and probed with antibodies against vWF (endothelium) or MYH11 (SMC). > 45 cells in 3 separate images per clone were quantified using ImageJ to determine % of cells that give rise to each lineage. **h)** MesoT in CDM -Activin A treated with VEGF generate mixtures of endothelial cells (vWF^+) and SMCs ($calponin^+$). Scale bar, 50 μm. **i,j)** Cells as in **(h)** were cultured on Matrigel for 12 days. Bright field images **(i)** of resulting vessel structures were probed with antibodies for αSMA and vWF and the nuclei counter stained with DAPI **(j)**. Scale bars, 50 μm.

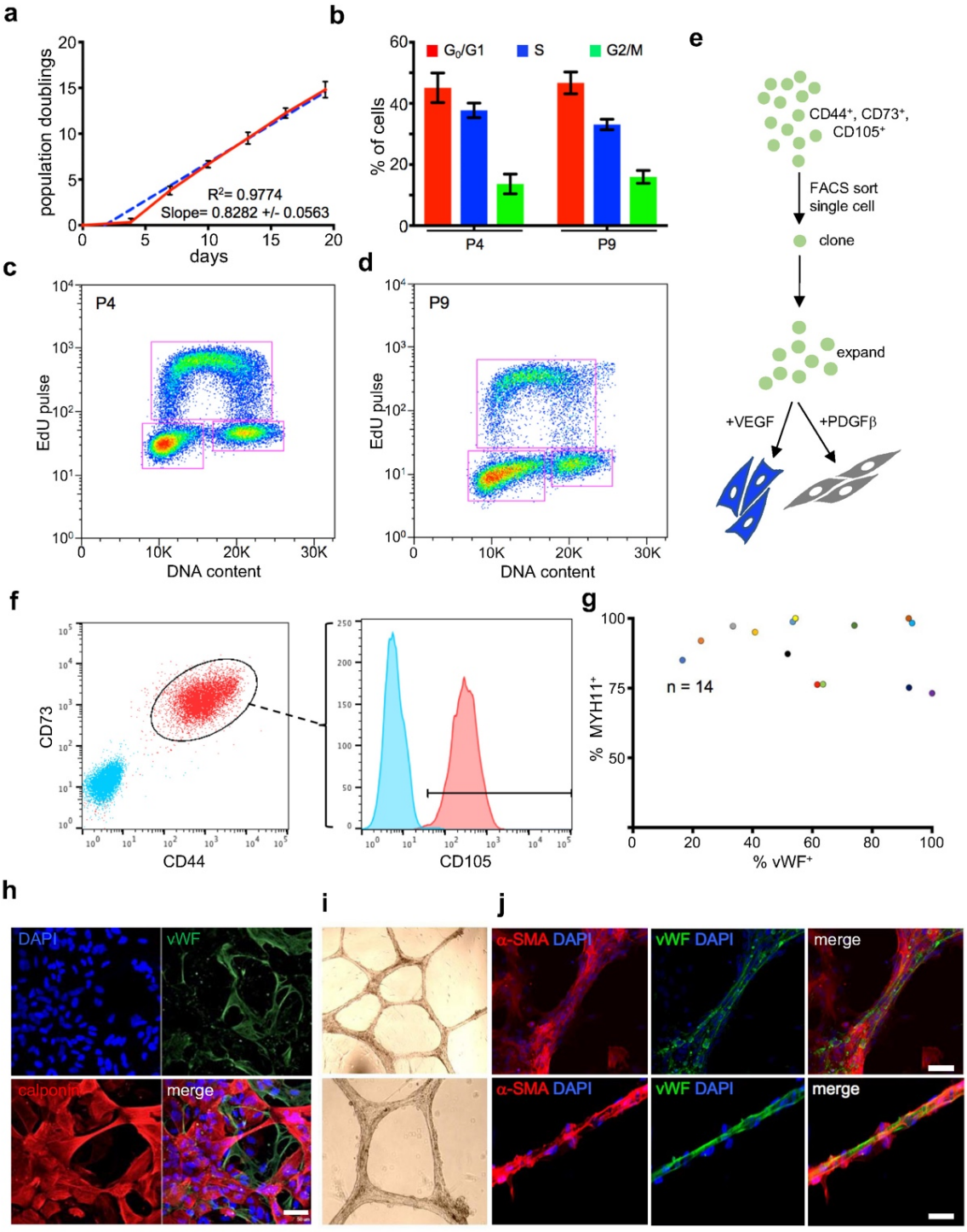
a
population doublings
days
R²= 0.9774
Slope= 0.8282 +/- 0.0563
b
% of cells
G0/G1
S
G2/M
P4
P9
c
P4
EdU pulse
DNA content
d
P9
EdU pulse
DNA content
e
CD44+, CD73+, CD105+
FACS sort single cell
clone
expand
+VEGF
+PDGFβ
f
CD73
CD44
CD105
g
% MYH11+
n = 14
% vWF+
h
DAPI
vWF
calponin
merge
i
j
α-SMA DAPI
vWF DAPI
merge

Figure 3.5 | MesoT cells incorporate into newly formed blood vessels in a neonatal mouse heart injury model.

a,b) Surgery on P0.5 mouse pups that includes ventricle apex resection. After resection, the damaged heart was overlaid with a 2 μl suspension of 1 x 10^6 DiO-labeled MesoTs **(b)** followed by suturing of the rib cage and chest wall. Micron bar, 1 mm. **c)** Cryo-section (10 μm) of a repaired mouse heart, 30 days post-injury. Tissue was probed with antibodies for αSMA, CD31, human Golgi antigen and DAPI. Scale bars, 50 μm. **d)** Repair zone showing a submesothelial blood vessel (bv) comprised of human αSMA^+ cells and human $CD31^+$ cells. Scale bars; top left, 20 μm; and other panels, 10 μm.

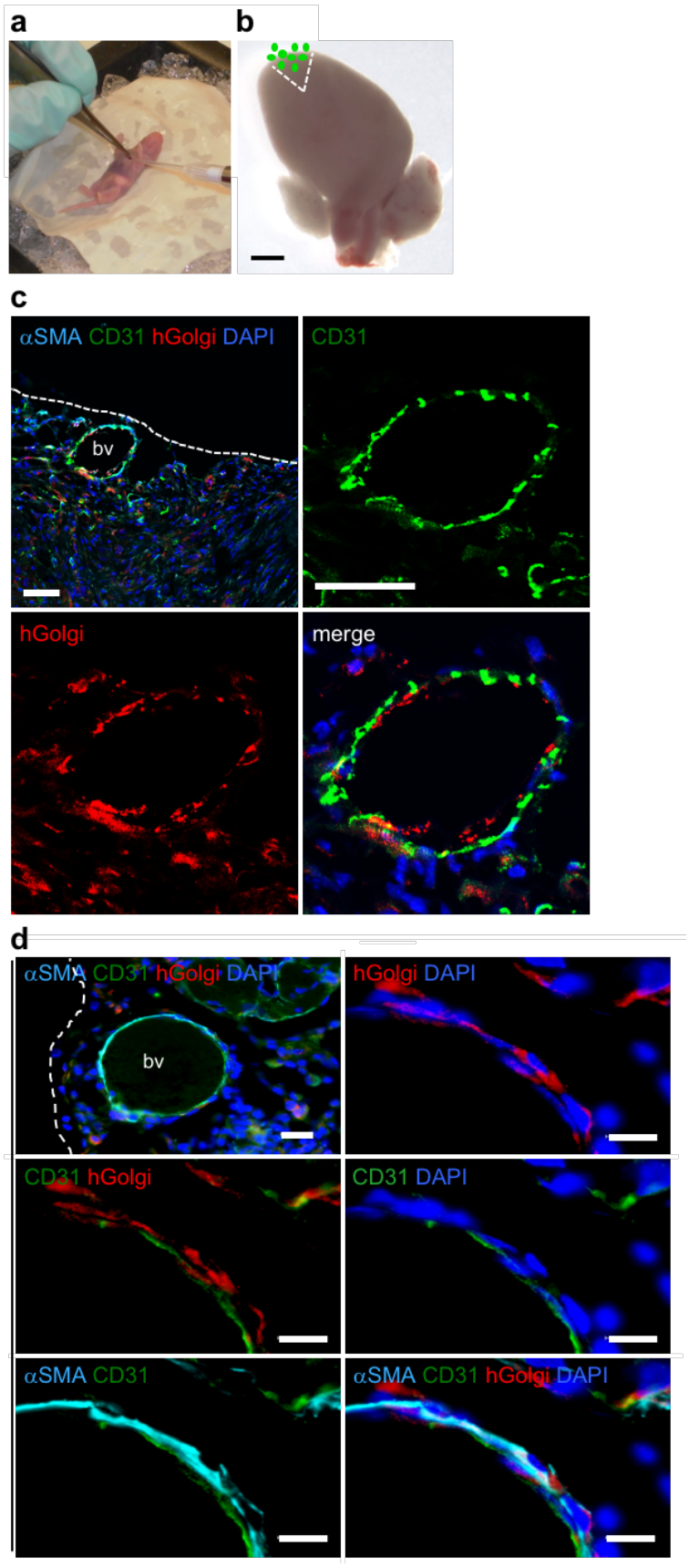
a
b
c
αSMA CD31 hGolgi DAPI
bv
CD31
hGolgi
merge
d
αSMA CD31 hGolgi DAPI
bv
hGolgi DAPI
CD31 hGolgi
CD31 DAPI
αSMA CD31
αSMA CD31 hGolgi DAPI

Figure 3.6 | Reperfusion of a decellularized biological scaffold with MesoT vascular progenitor cells repopulates the vascular network and forms functional invested vessels when transplanted *in vivo*.

a) Image of a decellularized rat jejunum and **(b,c)** injected with phenol red to contrast the vasculature before cell perfusion. **d)** MesoTs were perfused through the arterial and venous cannulas with (+VEGF) media. MTT assay imaging depicts reseeded vasculature with metabolically active cells after 28 days. Right panel is blowup of inset on left. Red lines mark representative vessels of various sizes. Micron bar, 1 mm. **e)** Vasculature derived by seeding MesoTs was stained human nuclear antigen (hNA) and DAPI. **f-h)** Vessels of small, medium and large diameter as in **(d)** were stained with antibodies against CD31 or αSMA. Scale bars, 100 μm. **i)** Vascular barrier integrity testing by perfusion with FITC-dextran. Left panel: bright field image before perfusion; Middle panel: intravital microscopy image of FITC-dextran retention after repeated perfusion and washing of the vascular network; Right panel: uptake of acetylated low-density lipoprotein (LDL, red). Nuclei were visualized with NucBlue™ Live ReadyProbes™. Scale bars, 100 μm. **j)** Light sheet microscopy image of vessel networks after fixation and staining with CD31 antibody. Scale bar, 400 μm. **k)** Reseeded vascular constructs were transplanted into 8-week-old immunodeficient female rats and anastomosed (white arrow) with the host circulatory system. **l)** Gross anatomical image of a transplanted graft after harvesting, showing the presence of host oxygenated blood and the absence of occlusion or leakage. **m-o)** Harvested grafts stained with antibodies for CD31 (red) and αSMA (green). Blood vessels of various sizes show a lining of endothelium and smooth muscle cells. Scale bars, 100 μm.

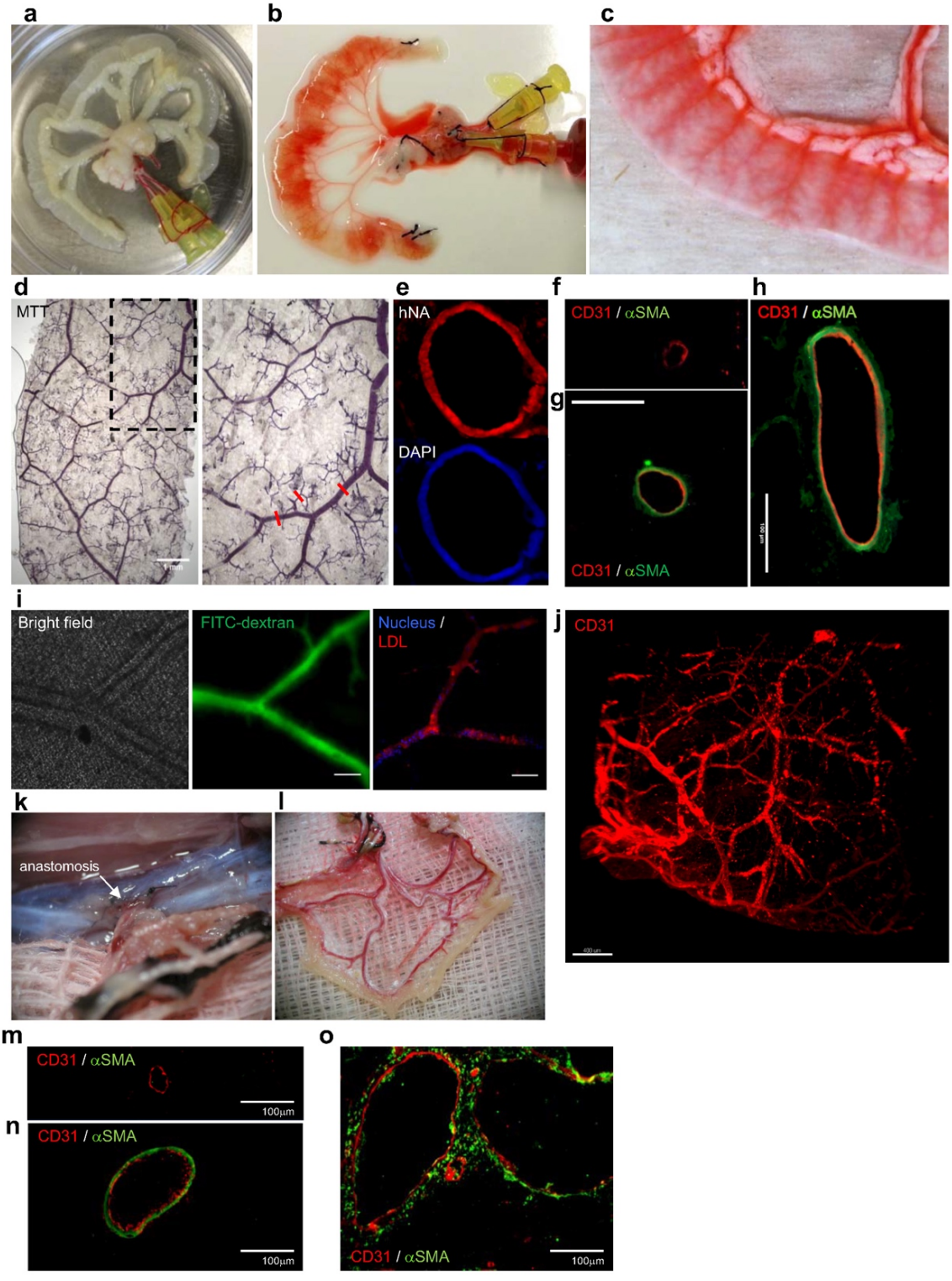
a
b
c
d
MTT
e
hNA
DAPI
f
CD31 / αSMA
g
CD31 / αSMA
h
CD31 / αSMA
i
Bright field
FITC-dextran
Nucleus /
LDL
j
CD31
k
anastomosis
l
m
CD31 / αSMA
100μm
n
CD31 / αSMA
100μm
o
CD31 / αSMA
100μm

Supplementary Figure 3.1 | Directed differentiation of hPSCs to MesoTs through a SplM intermediate.

a) hESC-derived (WA09) splanchnic mesoderm (SplM) cells generated after 4 days of culture in CDM supplemented with BMP4 (100 ng/ml) were fixed and stained with antibodies for ISL1, NKX2.5 and FLK1. Scale bars, 50 μm. **b)** Immunofluorescence analysis of K3 hiPSCs and hESCs (TE03, WA07 and WA01) cultured and stained as in **(a)**. Nuclei were counter stained with DAPI. Scale bars, 50 μm. **c)** qRT-PCR data showing fold-change of transcript levels for pluripotency markers (*NANOG*, *OCT4* and *SOX2*) in SplM and MesoTs relative to hESCs. TaqMan assays for each transcript were performed in technical triplicate and fold-change shown relative to hESCs (WA09) after normalization with 18S RNA. Error bars +/- standard deviation. **d)** Flow cytometry data of untreated hESCs (WA09), SplM and MesoT showing the absence of the pluripotent marker SOX2 (left plot) and presence of lineage specific marker ISL1 (middle plot) in SplM. As cells transition to MesoT, ISL1 is downregulated (right plot). **e)** Immunofluorescence of WA07, TE03 and K3 hiPSC lines after differentiation of SplM to MesoT followed by probing with WT1 and TBX18 antibodies. Nuclei were counter stained with DAPI. Scale bar, 50 μm. **f)** Flow cytometry pseudocolor plot of MesoT cells probed with antibodies for WT1 and TBX18. **g)** WA09-derived MesoT cells were fixed and probed with antibodies for lineage specific markers WT1 and TBX18. Nuclei were counterstained with DAPI. Right hand side is a magnification of the insets from left. Scale bars, 50 μm.

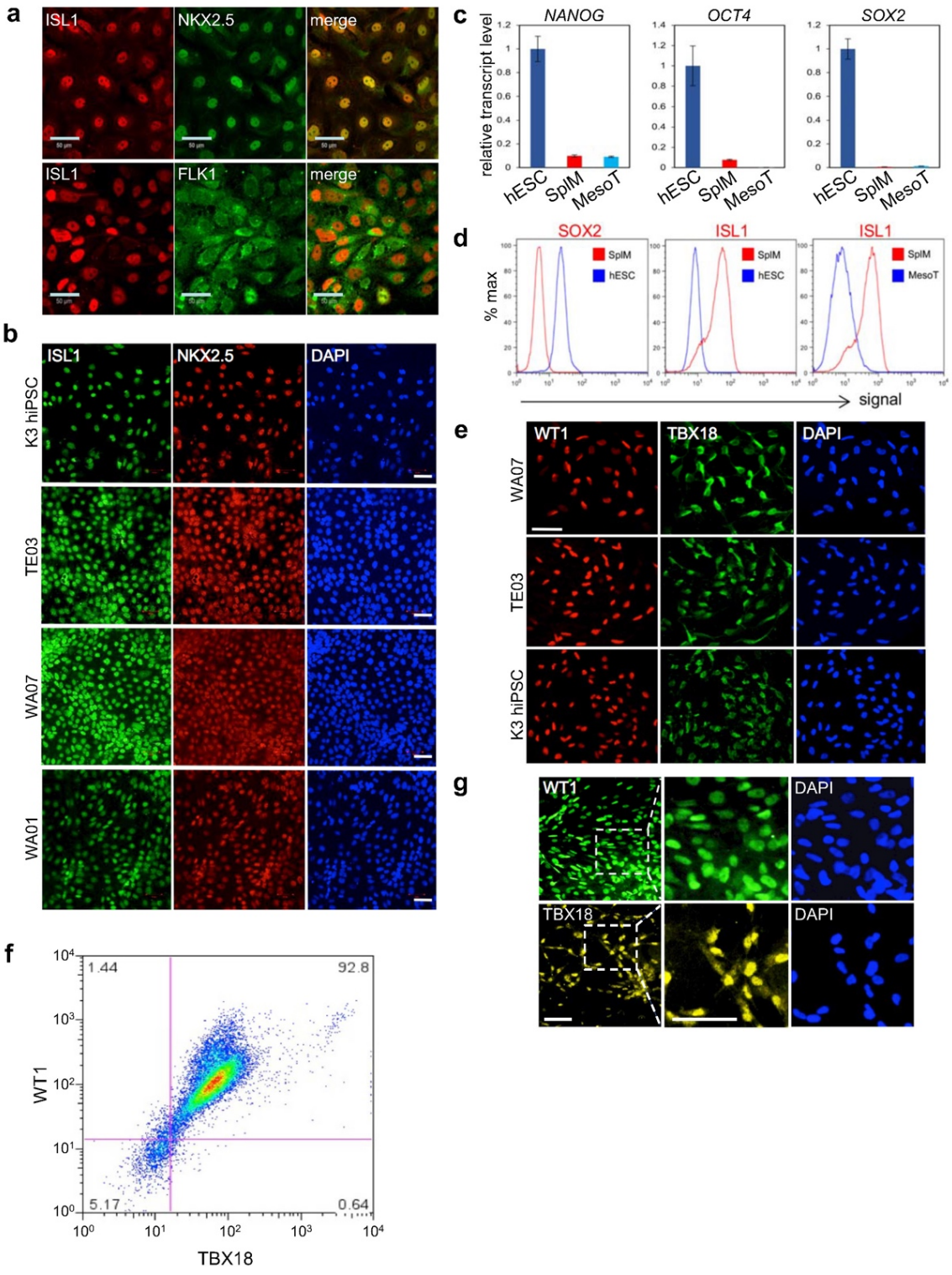
a
ISL1
NKX2.5
merge
ISL1
FLK1
merge
b
ISL1
NKX2.5
DAPI
K3 hiPSC
TE03
WA07
WA01
c
NANOG
OCT4
SOX2
relative transcript level
hESC
SplM
MesoT
d
SOX2
ISL1
ISL1
SplM
hESC
MesoT
% max
signal
e
WT1
TBX18
DAPI
WA07
TE03
K3 hiPSC
f
1.44
92.8
5.17
0.64
WT1
TBX18
g
WT1
DAPI
TBX18
DAPI

Supplementary Figure 3.2 | MesoT are a mesenchymal derivative of mesothelial cells generated from SplM.

a) Schematic showing the progression of splanchnic mesoderm (SplM) to mesothelium-like cells (MLCs) and then MesoTs. Removal and addition of growth factors and inhibitors are indicated above the arrows for each stage. **b)** qRT-PCR data showing fold-change of transcript levels for pluripotency (*OCT4, NANOG*), SplM (*ISL1* and *NKX2.5*) and mesothelium (*WT1, TBX18*, *TCF21 and MSLN*). TaqMan assays for each transcript were performed in technical triplicate and fold-change shown relative to untreated hESCs (WA09) after normalization with 18S RNA. Error bars +/- standard deviation. **c)** Immunofluorescence analysis of MLCs and MesoTs directly derived from MLCs. After EMT induction of MLCs **(a)**, cells become migratory but retain expression of mesothelial lineage markers. Cells were fixed and stained with antibodies against ISL1, NKX2.5, WT1, TBX18, E-cadherin (epithelial marker) and alpha smooth muscle actin (αSMA). Scale bars, 50 μm.

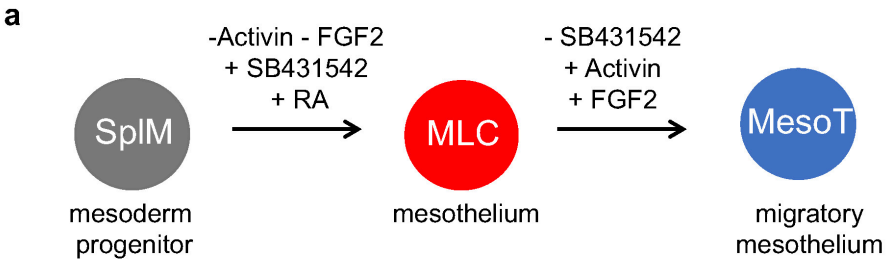
a
-Activin - FGF2
+ SB431542
+ RA
- SB431542
+ Activin
+ FGF2
SplM
MLC
MesoT
mesoderm progenitor
mesothelium
migratory mesothelium

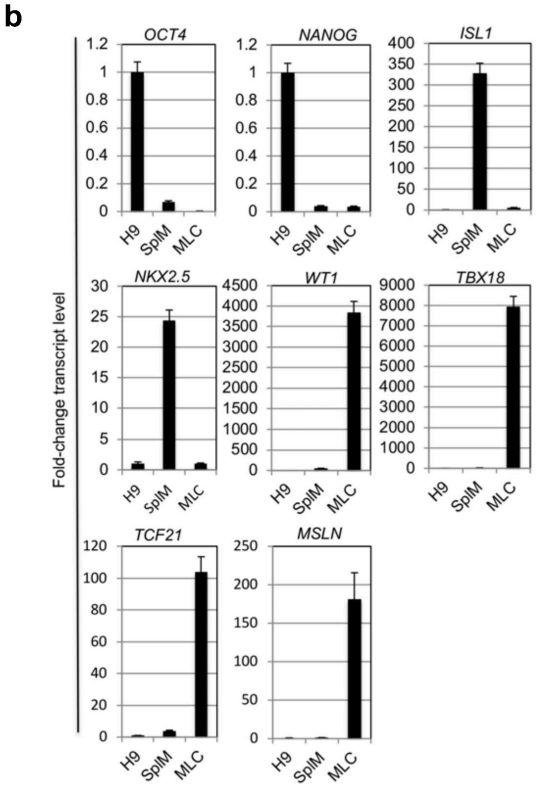
b
OCT4
NANOG
ISL1
NKX2.5
WT1
TBX18
TCF21
MSLN
Fold-change transcript level
H9
SplM
MLC

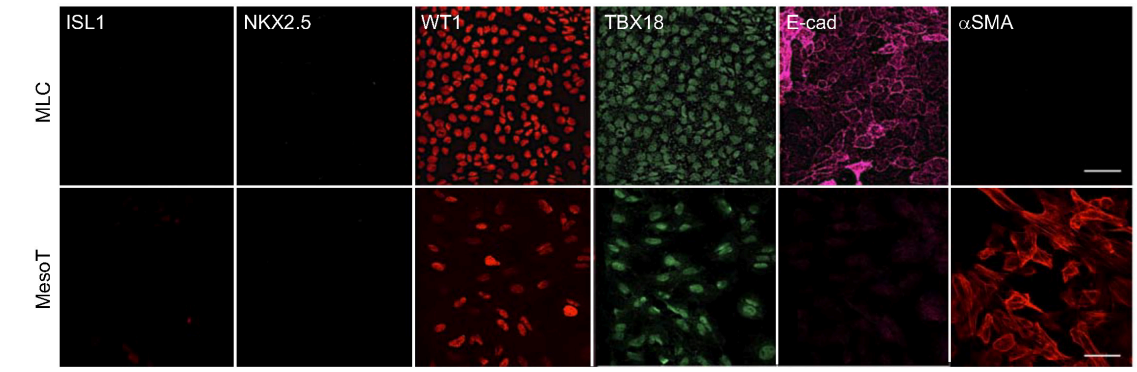
c
ISL1
NKX2.5
WT1
TBX18
E-cad
αSMA
MLC
MesoT

Supplementary Figure 3.3 | DNA methylation modules and Gene Ontology analysis.

a) Heatmap showing the relationship between cell type-specific DNA methylation modules (WA09 hPSCs, hPSC-derived splanchnic mesoderm, MesoTs and hPSC-derived cardiomyocytes). Module 9 comprises 1846 cytosines and is characteristic of MesoTs.

b,c) Gene Ontology analysis of genes analyzed in **Fig. 2d**.

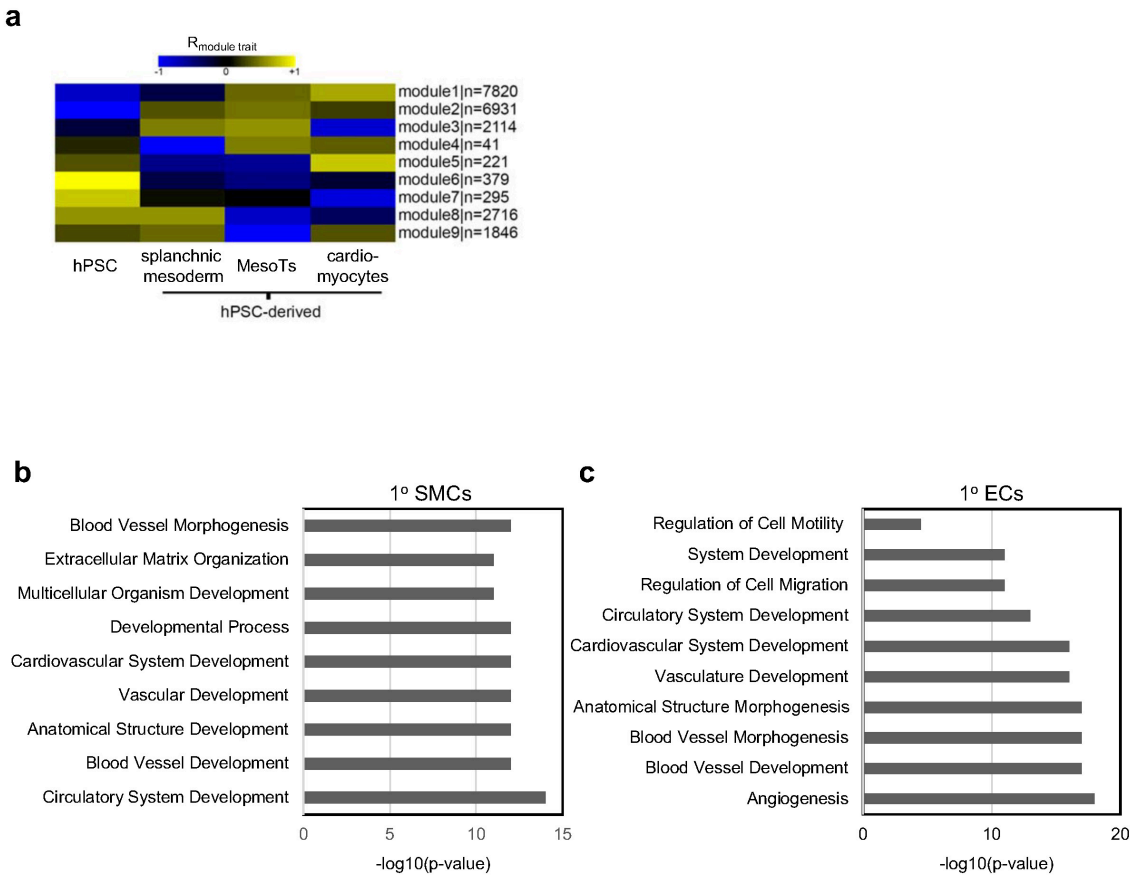
a
R module trait
-1
0
+1
module1|n=7820
module2|n=6931
module3|n=2114
module4|n=41
module5|n=221
module6|n=379
module7|n=295
module8|n=2716
module9|n=1846
hPSC
splanchnic mesoderm
MesoTs
cardio-myocytes
hPSC-derived
b
1° SMCs
Blood Vessel Morphogenesis
Extracellular Matrix Organization
Multicellular Organism Development
Developmental Process
Cardiovascular System Development
Vascular Development
Anatomical Structure Development
Blood Vessel Development
Circulatory System Development
0
5
10
15
-log10(p-value)
c
1° ECs
Regulation of Cell Motility
System Development
Regulation of Cell Migration
Circulatory System Development
Cardiovascular System Development
Vasculature Development
Anatomical Structure Morphogenesis
Blood Vessel Morphogenesis
Blood Vessel Development
Angiogenesis
0
10
20
-log10(p-value)

Supplementary Figure 3.4 | MesoT cells are negative for smooth muscle, endothelium and pericyte markers indicating no starting cell contamination.

a) Cells numbers at different stages of differentiation are shown. Cell number was counted at each stage after plating 1 million hESCs. **b)** Immunofluorescence of MesoT cells probed with antibodies for WT1, calponin, αSMA, vWF and MYH11. Nuclei were counterstained with DAPI. Scale bar, 50 μm. **c)** MesoT-derived SMCs were probed with antibodies for WT1, DDR2 and counterstained with DAPI. **d)** Flow cytometry histograms of MesoT cells probed with antibodies for CD31, NG2 and isotype control. **e)** Immunofluorescence of MesoT (FBS) cells after culturing with 2% FBS +VEGF (endothelium) or +PDGFβ (SMC). Cells were fixed and probed with antibodies against vWF or MYH11 and counter stained with DAPI. Scale bars, 50 μm.

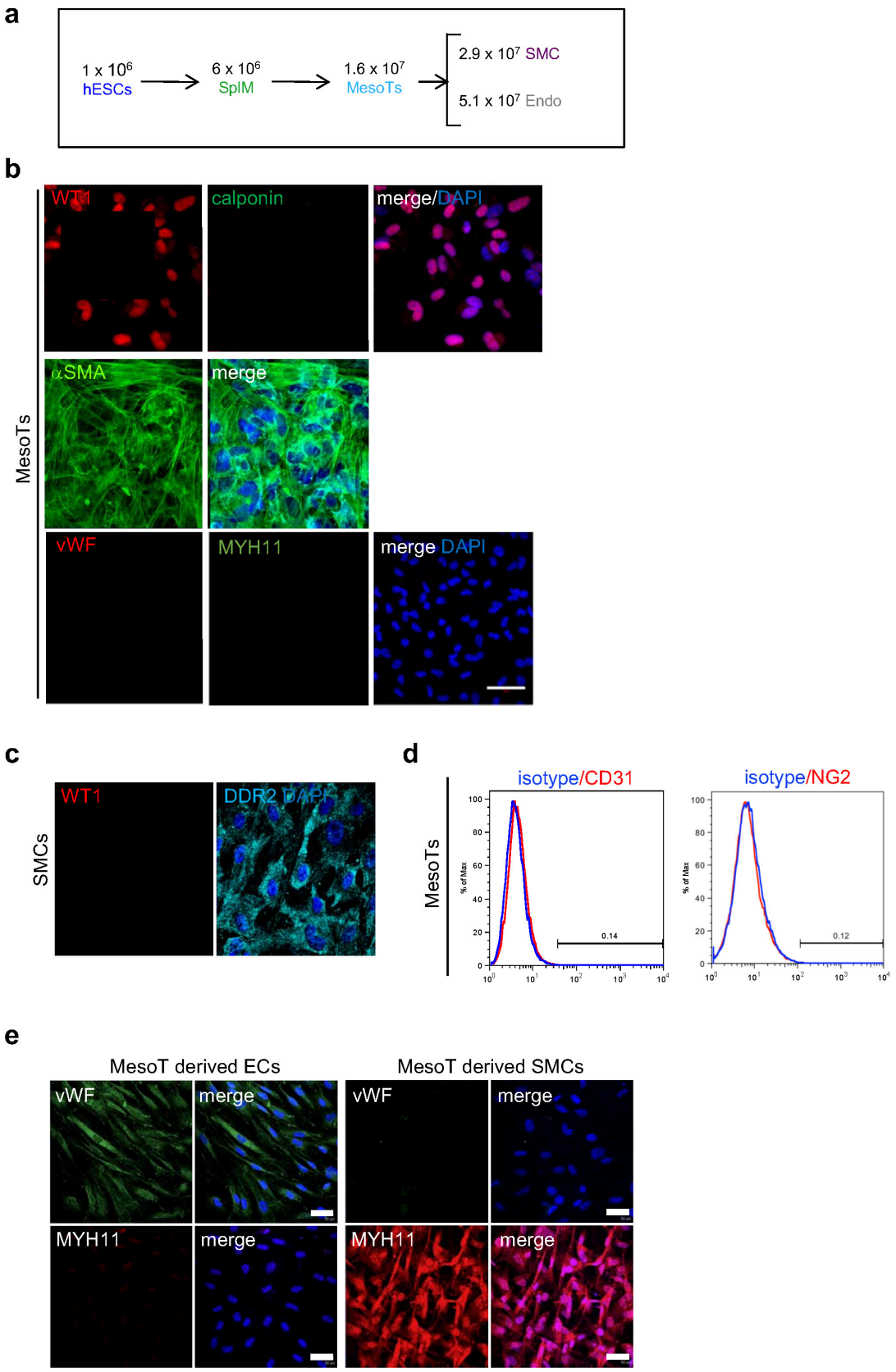
a
1 x 10^6 hESCs
6 x 10^6 SplM
1.6 x 10^7 MesoTs
2.9 x 10^7 SMC
5.1 x 10^7 Endo
b
MesoTs
WT1
calponin
merge/DAPI
αSMA
merge
vWF
MYH11
merge DAPI
c
SMCs
WT1
DDR2 DAPI
d
MesoTs
isotype/CD31
isotype/NG2
% of Max
0.14
0.12
e
MesoT derived ECs
MesoT derived SMCs
vWF
merge
MYH11
merge

Supplementary Figure 3.5 | MesoT cells attach to the mechanically injured neonatal mouse heart and contribute to new vessels linked to the host circulation.

a) Whole mount image of a mechanically injured heart 5 days after resecting part of the ventricle. **b)** DiO labeled MesoT human cells (green) were applied immediately after resection and attached to injured area. Micron bar, 1 mm. **c)** Blood vessel from **Fig. 5d** showing the presence of erythrocytes due to autofluorescence. Scale bar, 20 μm.

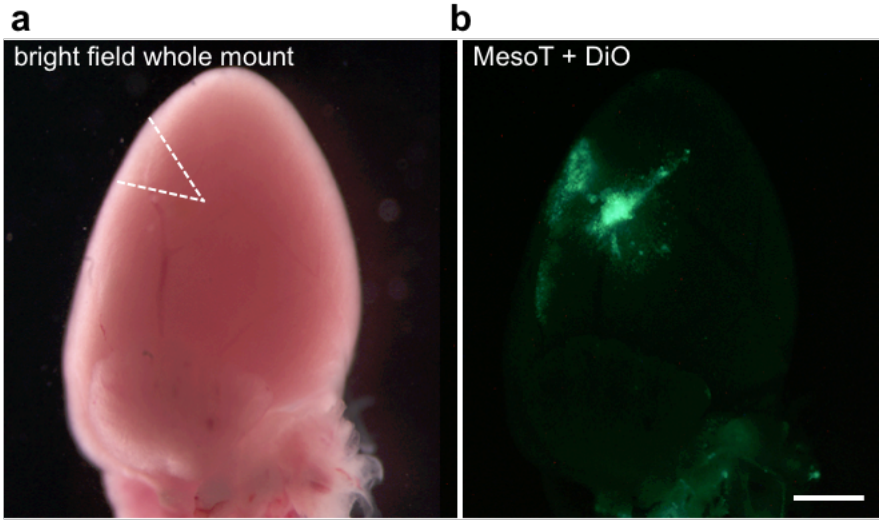
a
bright field whole mount
b
MesoT + DiO

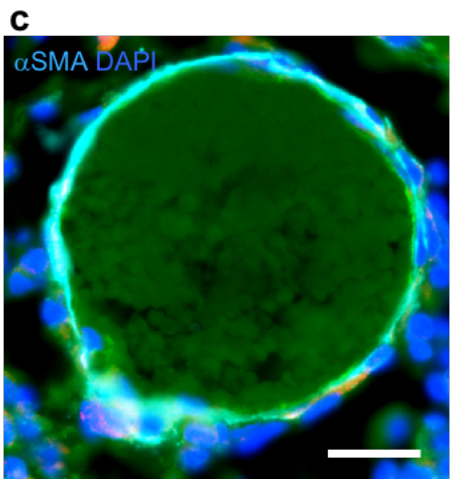
c
αSMA DAPI

Supplementary Figure 3.6 | MesoT cells successfully reseed vascular networks.

a) Cartoon schematic of bioreactor system to recellularize constructs with MesoT cells. **b)** MTT assay of a decellularized construct showing the absence of viable cells. **c)** Left panel; bright field image before FITC-dextran perfusion. Time lapse images immediately following perfusion of 1x injected constructs, FITC-dextran leaked into the lumen showing the lack of tight barriers after 28 days. Scale bar = 100 μm. **d,e)** Lightsheet microscopy images as in Fig. 6j showing CD31+ endothelium lining the scaffold after 28 days. Scale bars = 500 μm. **f)** Lightsheet microscopy image showing NG2+ pericytes lining vessels. Scale bar = 150 μm. **g)** Gross anatomy examination as in Fig. 6l after harvesting.

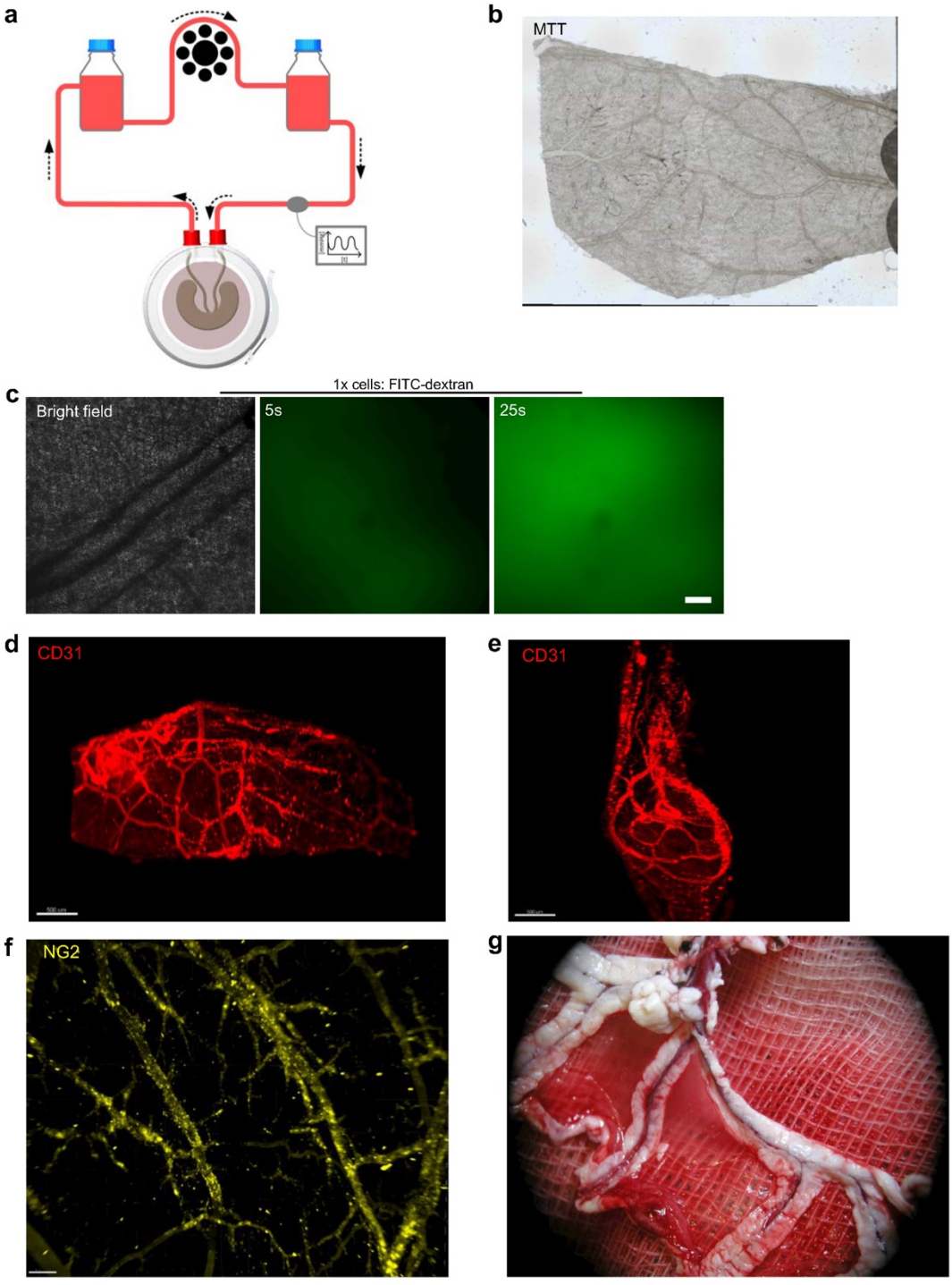
a
b
MTT
c
1x cells: FITC-dextran
Bright field
5s
25s
d
CD31
e
CD31
f
NG2
g

References

1. Mutsaers, S. E. & Wilkosz, S. Structure and function of mesothelial cells. *Cancer Treat. Res.* **134**, 1-19 (2007).
2. Zangi, L. *et al.* Modified mRNA directs the fate of heart progenitor cells and induces vascular regeneration after myocardial infarction. *Nat. Biotechnol.* **31,** 898–907 (2013).
3. Rinkevich, Y. *et al.* Identification and prospective isolation of a mesothelial precursor lineage giving rise to smooth muscle cells and fibroblasts for mammalian internal organs, and their vasculature. *Nat. Cell Biol.* **14,** 1251–1260 (2012).
4. Que, J. *et al.* Mesothelium contributes to vascular smooth muscle and mesenchyme during lung development. *Proc. Natl. Acad. Sci. USA* **105,** 16626–16630 (2008).
5. Cano, E., Carmona, R. & Muñoz-Chapuli, R. Wt1-expressing progenitors contribute to multiple tissues in the developing lung. *Am. J. Physiol. Lung Cell Mol. Physiol.* **305,** L322–32 (2013).
6. Wilm, B., Ipenberg, A., Hastie, N. D., Burch, J. B. E. & Bader, D. M. The serosal mesothelium is a major source of smooth muscle cells of the gut vasculature. *Development* **132,** 5317–5328 (2005).
7. Dixit, R., Ai, X. & Fine, A. Derivation of lung mesenchymal lineages from the fetal mesothelium requires hedgehog signaling for mesothelial cell entry. *Development* **140,** 4398–4406 (2013).

8. Asahina, K. *et al.* Mesenchymal origin of hepatic stellate cells, submesothelial cells, and perivascular mesenchymal cells during mouse liver development. *Hepatology* **49,** 998–1011 (2009).

9. Smith, C. L., Baek, S. T., Sung, C. Y. & Tallquist, M. D. Epicardial-derived cell epithelial-to-mesenchymal transition and fate specification require PDGF receptor signaling. *Circ. Res.* **108,** e15–26 (2011).

10. Chong, J. J. H. *et al.* Adult Cardiac-Resident MSC-like Stem Cells with a Proepicardial Origin. *Cell Stem Cell* **9,** 527–540 (2011).

11. Smart, N. *et al.* De novo cardiomyocytes from within the activated adult heart after injury. *Nature* **474,** 640–644 (2011).

12. Kikuchi, K. *et al.* tcf21+ epicardial cells adopt non-myocardial fates during zebrafish heart development and regeneration. *Development* **138,** 2895–2902 (2011).

13. Elmadbouh, I. *et al.* Mesothelial cell transplantation in the infarct scar induces neovascularization and improves heart function. *Cardiovasc. Res.* **68,** 307–317 (2005).

14. Lucas, P. A. Stem cells for mesothelial repair: an understudied modality. *Int. J. Artif. Organs* **30,** 550–556 (2007).

15. Shelton, E. L. & Bader, D. M. Thymosin β4 mobilizes mesothelial cells for blood vessel repair. *Ann. N. Y. Acad. Sci.* **1269,** 125–130 (2012).

16. van Wijk, B., Gunst, Q. D., Moorman, A. F. M. & van den Hoff, M. J. B. Cardiac regeneration from activated epicardium. *PLoS One* **7,** e44692 (2012).

17. Porrello, E. R. *et al.* Transient regenerative potential of the neonatal mouse heart. *Science* **331,** 1078–1080 (2011).

18. Liu, Q. *et al.* Epicardium-to-fat transition in injured heart. *Cell Res.* **24,** 1367–1369 (2014).

19. Cheung, C., Bernardo, A. S., Trotter, M. W. B., Pedersen, R. A. & Sinha, S. Generation of human vascular smooth muscle subtypes provides insight into embryological origin-dependent disease susceptibility. *Nat. Biotechnol.* **30,** 165–173 (2012).

20. Patsch, C. *et al.* Generation of vascular endothelial and smooth muscle cells from human pluripotent stem cells. *Nat. Cell Biol.* **17,** 994–1003 (2015).

21. James, D. *et al.* Expansion and maintenance of human embryonic stem cell-derived endothelial cells by TGFbeta inhibition is Id1 dependent. *Nat. Biotechnol.* **28,** 161–166 (2010).

22. Nagai, H. *et al.* Metamorphosis of mesothelial cells with active horizontal motility in tissue culture. *Sci. Rep.* **3,** 1144 (2013).

23. Tian, X., Pu, W. T. & Zhou, B. Cellular origin and developmental program of coronary angiogenesis. *Circ. Res.* **116,** 515–530 (2015).

24. Rada-Iglesias, A. *et al.* A unique chromatin signature uncovers early developmental enhancers in humans. *Nature* **470,** 279–283 (2011).

25. Creyghton, M. P. *et al.* Histone H3K27ac separates active from poised enhancers and predicts developmental state. *Proc. Natl. Acad. Sci. USA* **107,** 21931–21936 (2010).

26. Mellgren, A. M. *et al.* Platelet-derived growth factor receptor beta signaling is required for efficient epicardial cell migration and development of two distinct coronary vascular smooth muscle cell populations. *Circ. Res.* **103,** 1393–1401 (2008).

27. Bryant, D. M. *et al.* A systematic analysis of neonatal mouse heart regeneration after apical resection. *J. Mol. Cell. Cardiol.* **79,** 315–318 (2015).

28. Andersen, D. C., Ganesalingam, S., Jensen, C. H. & Sheikh, S. P. Do neonatal mouse hearts regenerate following heart apex resection? *Stem Cell Rep.* **2,** 406–413 (2014).

29. Lepilina, A. *et al.* A dynamic epicardial injury response supports progenitor cell activity during zebrafish heart regeneration. *Cell* **127,** 607–619 (2006).

30. Winters, N. I., Williams, A. M. & Bader, D. M. Resident progenitors, not exogenous migratory cells, generate the majority of visceral mesothelium in organogenesis. *Dev. Biol.* **391,** 125–132 (2014).

31. Iyer, D. *et al.* Robust derivation of epicardium and its differentiated smooth muscle cell progeny from human pluripotent stem cells. *Development* **142,** 1528–1541 (2015).

32. Witty, A. D. *et al.* Generation of the epicardial lineage from human pluripotent stem cells. *Nat. Biotechnol.* **32,** 1026–1035 (2014).

33. Katz, T. C. *et al.* Distinct compartments of the proepicardial organ give rise to coronary vascular endothelial cells. *Dev. Cell* **22,** 639–650 (2012).

34. Cao, J. *et al.* Single epicardial cell transcriptome sequencing identifies Caveolin 1 as an essential factor in zebrafish heart regeneration. *Development* **143,** 232–243 (2016).

35. Singh, M. K. & Epstein, J. A. Epicardium-derived cardiac mesenchymal stem cells: expanding the outer limit of heart repair. *Circ. Res.* **110,** 904–906 (2012).

36. Gittenberger-de Groot, A. C., Winter, E. M. & Poelmann, R. E. Epicardium-derived cells (EPDCs) in development, cardiac disease and repair of ischemia. *J. Cell. Mol. Med.* **14,** 1056–1060 (2010).

37. Pennisi, D. J. Towards Consensus on Coronary Vessel Development: Coronary Arterial Endothelial Cells Derive Primarily From the Sinus venosus During Embryogenesis. *Circ. Res.* **118,** 1861–1862 (2016).

38. Cano, E. *et al.* Extracardiac septum transversum/proepicardial endothelial cells pattern embryonic coronary arterio-venous connections. *Proc. Natl. Acad. Sci. USA* **113,** 656–661 (2016).

39. Chen, H. I. *et al.* The sinus venosus contributes to coronary vasculature through VEGFC-stimulated angiogenesis. *Development* **141,** 4500–4512 (2014).

40. Pérez Pomares, J. M. & la Pompa, de, J. L. Signaling during epicardium and coronary vessel development. *Circ. Res.* **109,** 1429–1442 (2011).

41. Palmquist-Gomes, P., Guadix, J. A. & Pérez-Pomares, J. M. Avian embryonic coronary arterio-venous patterning involves the contribution of different endothelial and endocardial cell populations. *Dev. Dyn.* **247,** 686–698 (2018).

42. Doi, R. *et al.* Transplantation of bioengineered rat lungs recellularized with endothelial and adipose-derived stromal cells. *Sci. Rep.* **7,** 8447 (2017).

43. Ren, X. *et al.* Engineering pulmonary vasculature in decellularized rat and human lungs. *Nat. Biotechnol.* **33,** 1097–1102 (2015).

44. Drews, J. D., Miyachi, H. & Shinoka, T. Tissue-engineered vascular grafts for congenital cardiac disease: Clinical experience and current status. *Trends Cardiovasc. Med.* **27,** 521–531 (2017).

45. Villalona, G. A. *et al.* Cell-seeding techniques in vascular tissue engineering. *Tissue Eng Part B Rev* **16,** 341–350 (2010).

46. Lee, Y.-U. *et al.* Rational design of an improved tissue-engineered vascular graft: determining the optimal cell dose and incubation time. *Regen. Med.* **11,** 159–167 (2016).

47. Asahara, T. *et al.* Isolation of putative progenitor endothelial cells for angiogenesis. *Science* **275,** 964–967 (1997).

48. Alphonse, R. S. *et al.* The isolation and culture of endothelial colony-forming cells from human and rat lungs. *Nat. Protoc.* **10,** 1697–1708 (2015).

49. Prasain, N. *et al.* Differentiation of human pluripotent stem cells to cells similar to cord-blood endothelial colony-forming cells. *Nat. Biotechnol.* **32,** 1151–1157 (2014).

CHAPTER 4

DETAILED EXPERIMENTAL PROCEDURES

Materials and methods

Cell Culture and Differentiation

Maintenance of pluripotent cells[1] and differentiation to splanchnic mesoderm[2] was as previously described. Briefly, WA09, WA07, TE03 (WiCell) hESCs and K3 hiPSCs[3] were maintained in chemically-defined media (CDM)[4] consisting of DMEM/F12 w/o glutamine supplemented with 1x nonessential amino acids, 1x antimycotic/antibiotic, 1x trace elements A, B and C, 2 mM L-alanyl-L-glutamine (all from Corning), 10 μg/ml transferrin (HOLO), human plasma, tissue culture grade (Athens Research and Technology), 2% Probumin® bovine serum albumin life science grade (EMD Millipore), 0.1 mM β-mercaptoethanol (Gibco), 50 μg/mL ascorbic acid (Sigma), 10 ng/ml rhHeregulin β-1 (Peprotech), 200 ng/ml LONG® R3 IGF-I human (Sigma), 10 ng/ml rhActivin A and 8 ng/ml rhFGF basic (both from R&D Systems) on 1:200 Geltrex (Thermo Fisher) coated plates. Cells were passaged with Accutase (Innovative Cell Technologies). For splanchnic mesoderm (SplM) induction, hPSCs were passaged as above and reseeded at 5 x 10^4 cells/cm^2 (WA09) or 1 x 10^5 cells/cm^2 (WA01, WA07, TE03 and K3) onto Geltrex coated plates into CDM supplemented with 25 ng/ml rhWNT3a and 100 ng/ml rhBMP4 (both from R&D Systems) for 4 days with media changed daily. For migratory mesothelium (MesoT) induction, CDM is supplemented

with 25 ng/ml rhWNT3a, 50 ng/ml rhBMP4 and 4 μM all-trans retinoic acid (Sigma) for an additional 14-18 days. To self-renew MesoT (FBS), cells were passaged with collagenase type IV (800 units/ml) (Thermo Fisher) followed by 1x TrypLE Select (Thermo Fisher) and cultured with 10% fetal bovine serum (Atlanta Biologicals), Minimal Essential Media, Alpha (Corning), 1x antibiotic/antimycotic, 2 mM L-alanyl-L-glutamine and 8 ng/ml FGF2 at an initial seeding density of 5 x 10^4/cm^2 on plastic then 1 x 10^4/cm^2 for subsequent passages using 1x TrypLE Select. Media was changed every day. For generation of mesothelium-like cells (MLCs), SplM is passed with 1x TrypLE select then replated at 1.5 x 10^5 cells/cm^2 in CDM -FGF2 -Activin A +25 ng/ml rhWNT3a +50 ng/ml BMP4 +20 μM SB431542 +4 μM all-trans retinoic acid for 18 days with media changed daily.

MesoTs were passaged and reseeded at a density of 1.5 x 10^5/cm^2 on Geltrex coated plates. Activin A was removed from CDM for all vascular lineages differentiations and supplemented with the following: 50 ng/ml rhVEGF-A_{165} (R&D Systems) and 20 μM SB431542 (Tocris) for endothelial cell differentiations; 50 ng/ml PDGF-ββ (R&D Systems) for smooth muscle cell (SMC) differentiations for 12 days with media changed every other day. Removal of SB431542 from endothelial cell media was used to generate mixtures of endothelial cells and smooth muscle cells.

Immunofluorescence analysis of fixed cells

Immunofluorescence analysis was performed on 4% paraformaldehyde-fixed cells (10 min) in the presence of 10% donkey serum and 0.25% Triton X-100 followed by visualization using 2.5% donkey serum in PBS with fluorescent conjugated secondary

antibodies. Primary antibodies were incubated overnight at 4°C followed by conjugated secondary antibodies for 1 hour at room temperature (RT) in the dark. Nuclei were counterstained with 4′,6-Diamidino-2-phenylindole dihydrochloride (DAPI, Sigma) for 5 min and cover slips were affixed with ProLong Diamond Antifade (Thermo Fisher). Fluorescent cells were visualized on a Leica DM6000 B and BioTek Lionheart FX. Confocal images were obtained on an Olympus FV1200 laser scanning confocal microscope. All antibodies are listed in **Table 1 and Table 2**.

qRT-PCR

mRNA was isolated using RNeasy kit (Qiagen). cDNA was made using iSCRIPT cDNA kit (Bio-Rad) and qRT-PCR was performed using TaqMan Universal PCR Master Mix No AmpErase UNG and TaqMan Primers (both from Thermo Fisher) on a ViiA7 Real-Time PCR System (Life Technologies). TaqMan probe mixes are listed in **Table 3**.

Flow cytometry, cell cycle analysis and clonal analysis

Cells were collected as single cell suspensions following removal from the culture as noted above then analyzed by flow cytometry using a CyAn ADP (Beckman Coulter, Hialeah, Florida). Cells were stained with specific flow antibodies per manufacturer recommendations with isotype controls. Intracellular markers were analyzed using Flow Cytometry Permeabilization/Wash Buffer I (1x) (R&D Systems). Cell cycle analysis of MesoT cells was performed using a Click-iT™ Plus EdU Alexa Fluor™ 647 Flow Cytometry Assay Kit (Invitrogen) with 1 hour incubation. Population doublings were calculated using the following equation[5]:

$$\frac{\log \frac{End\ Cell\ Number}{Starting\ Cell\ Number}}{\log 2}$$

For clonal analysis, $CD44^{+}/CD73^{+}/CD105^{+}$ MesoT cells were single cell sorted onto 96 well plates (VWR) using 50/50 fresh and preconditioned media with a MoFlo XDP sorter (Beckman Coulter, Hialeah, Florida). After amplification, cells were passaged to downstream lineages using 2% fetal bovine serum, Minimal Essential Media, Alpha, 1x antibiotic/antimycotic, 2 mM L-alanyl-L-glutamine and 50 ng/ml rhVEGF-A_{165} (endothelium) or 50 ng/ml PDGF-ββ (smooth muscle). Multipotency was assessed by confocal imaging on an Olympus FV1200 confocal microscope and quantified with ImageJ software (NIH https://imagej.nih.gov/ij/). All flow and sorting analysis used FlowJo software (Treestar, Inc., Ashland, Oregon).

Isolation of embryonic mouse mesothelium

Wt1$^{creERT2/+}$ *Rosa26*$^{tdT/+}$ embryonic mice were generated by crossing *Wt1*$^{creERT2/+}$ mice[6] with a knock-in of tamoxifen inducible cre-recombinase in the Wt1 locus (Jackson Laboratory Stock #010912) and Rosa26$^{tdT/tdT}$ (Jackson Laboratory Stock #007914) mice with a *loxP*-flanked STOP cassette preventing transcription of a CAG promoter-driven red fluorescent protein variant, tdTomato[7]. At E12.5, pregnant dams were injected with 300 µl of 10 mg/ml tamoxifen/corn oil solution intra-peritoneally at 24 hour intervals for three consecutive days. Embryos were harvested at E15.5 and the heart, lung, liver and gut were carefully isolated using sterile technique. The outer mesothelial layer was digested by exposing intact organs to a dissociation buffer containing 1 mg/ml collagenase IV and 0.05% trypsin as described previously[8]. Briefly, the intact organs

were repeatedly digested (7-8 times) in collagenase IV-trypsin dissociation buffer at 6-7 min intervals on a 37°C shaker and the supernatants from each digest neutralized with horse serum, pooled and filtered through a 70 μM nylon mesh. Digested samples were suspended in FACS buffer (0.2% BSA in PBS). tdTomato$^+$ cell fractions were sorted using a MoFlo XDP and RNA was extracted for differential gene expression analysis.

RNA-seq analysis

RNA from tdTomato$^+$ fractions along with RNA from hESC-derived MesoT and MLCs were extracted with Trizol (Invitrogen) and purified with RNeasy mini kit (Qiagen) according to the manufacturer's instructions. RNA yield was determined using the NanoDrop ND-1000 spectrophotometer (NanoDrop Technologies) and purified RNA (1 μg) from each sample was submitted to the Hudson Alpha Institute (Huntsville, Alabama) for polyA$^+$ RNA sequencing (HiSeq v4 50 PE, 25 million reads per sample) and deposited under GSE113090. Additional raw data for human adult and fetal tissues were downloaded from the Sequence Read Archive (ERP003613, SRP001371) while additional mouse adult and fetal tissues were downloaded from ENCODE and the Sequence Read Archive (SRP049248, SRP018511). When necessary, *.sra formatted data were converted to the *.fastq format using the SRA Toolkit (version 2.4.1). Data quality was assessed using FastQC (version 0.10.1) before being mapped to known Ensemble genes (GRCh37/NCBIM37) using Tophat2 (version 2.0.13). Raw read counts for each gene were obtained using Subread (version 1.4.2).

Raw mouse and human read count data were read into R and combined into species specific data frames for differential expression analyses using linear modeling

strategies. The mouse sample set was comprised of four FACS-sorted mesothelium samples and replicated samples from 18 mouse tissues (40 total samples). The human sample set was comprised of 2 replicates of hPSC-derived MLCs, 4 replicates of hPSC-derived MesoT, and replicated samples from 25 human tissues (62 total samples). The RNA-seq expression sets were filtered to include genes having at least 5 reads in 2 or more samples (n_{mouse}=18836, n_{human}=21761). Raw read counts were normalized using the trimmed mean of M-values (TMM) method (PMID:20196867) and precision weights were calculated using voom (PMID:24485249) prior to differential analysis using the Limma empirical Bayes analysis pipeline (PMID:16646809). Mouse and human mesothelium gene expression signatures were identified by a series of comparisons between sample groups. Briefly, mesothelium samples (independently for epithelial and mesenchymal human forms) were first compared to all tissue sample groups together as a single group ("*vs_Rest*"; n_{mouse}=18, n_{human}=25), to the adult tissue sample groups together as a single group ("*vs_Adult*"; n_{mouse}=16, n_{human}=18), to the fetal tissue sample groups together as a single group ("*vs_Fetal*"; n_{mouse}=6, n_{human}=7), and to each of the tissue sample groups, independently (n_{mouse}=18, n_{human}=25). Two criteria were set in order for a candidate to be classified as a mesothelium signature gene. First, the gene had to be consistently expressed at either higher or lower levels in each of the "*vs_Rest*", "*vs_Adult*"*, and "vs_Fetal"* comparisons at FDR <= 0.05. Secondly, the gene had to also be consistently enriched or depleted in at least 70% of the targeted tissue comparisons (n_{mouse}>=12, n_{human}>=17) at FDR <= 0.05. Gene ranks were determined by sorting the genes according to the number of significant targeted tissue comparisons in descending order and, secondarily, the "*vs_Rest"* FDR value in ascending order. Rank percentiles

were determined in the context of all detected genes in that species (n_{mouse}= 18836, n_{human}=21761).

In order to determine whether the observed patterns of differential expression were conserved, a list of Mouse:Human orthologs was downloaded from www.genenames.org/cgi-bin/hcop.pl and processed to contain only ensemble gene IDs and gene names. Conservation ranks ("*orthoRANK.Epithelial*", "*orthoRANK.Mesenchymal*") were assigned to each conserved gene by averaging the percentile rank of each gene from the mouse and human comparisons.

Principal component analysis

RNA sequencing for two biological replicates of WA09 (hESCs), hESC-derived SplM, MesoT and hPSC-derived endothelial cells (ECs) and 1 replicate of hESC-derived smooth muscle cells (SMCs) was performed as described above. MesoT and smooth muscle cells were deposited under GSE113090. hESCs, SplM, fetal tissue and primary cell datasets were obtained from GSE101655, GSM2229922, GSE18927, GSM2227052 and GSM2288409, respectively. Raw data were aligned to human reference genome (hg19) using HIAST2 (version 2.1.0) with default parameters. Aligned reads were sorted with Samtools (version 1.3.1) and the number of reads mapping to each gene were counted by HTseq (version 0.6.1p1). All counting files from HTseq were imported into R studio (version 1.1.423). In order to generate PCA plot, data were pre-processed using Limma edgeR to normalize sequencing depth and gene expression distributions as well as remove low counts. PCA plot was made by Glimma using top 20% genes.

DNA methylation analysis

Bisulfite conversion was performed using the EZ DNA Methylation Kit (Zymo Research) according to the manufacturer's instructions. Whole genome amplification, fragmentation and preparation of the DNA for hybridization were performed using the Infinium HumanMethylation450 BeadChip kit (Illumina) as described in the manufacturer's protocol. Illumina IDATS were read directly into R and normalized using Subset-quantile within array normalization (PMID:22703947). Dynamic methylation analyses were performed using Limma in R. Briefly, triplicate MesoT samples were fit to a linear model along with undifferentiated hPSC, hPSC-derived SplM and hPSC-derived cardiomyocytes (all biological duplicates). Dynamic methylation loci were identified by selecting probes with FDR <= 0.01 in a targeted t-test comparing MesoT to undifferentiated hPSCs. These loci were further filtered by removing probes where the maximum difference in Beta values was < 0.3 between any of the sample group averages used to fit the linear model (n= 22561). DNA methylation modules were identified using weighted gene correlation network analysis in R (WGCNA, PMID:19114008).

ChIP-seq and Gene Ontology Analysis

ChIP-seq was performed as previously described[9]. Briefly, MesoT cells were chemically crosslinked with 1% formaldehyde (Thermo Scientific) for 10 min at room temperature, followed by quenching with 2.5 M glycine for 5 min. Samples were rinsed with cold 1X PBS once, harvested by centrifugation and stored at -80°C before use. Cross linked DNA was fragmented by sonication on a Covaris S220 with 140V peak power, a duty factor of 5 and 200 cycles for 10 min. H3K4 mono-methylation (Abcam)

and H3K27 acetylation (Abcam) antibodies were incubated with 50 µl Protein G Dynabeads (Invitrogen, 10004D) on a shaker at 4°C for 2 hours. Fragmented DNA, antibodies and beads were then incubated together on a shaker at 4°C overnight, approximately 5 million cells per reaction. Cross-linking was reversed by adding 20 mg/ml Proteinase K at 55°C for 30-40 min followed by incubation at 65°C for 8 hours. The final library was submitted to Hudson Alpha Institute for 50bp single-end sequencing. For each sample, ~25 M reads were obtained and input samples were used as controls. MesoT H3K4me1 and H3K27ac ChIP-seq data was deposited under GEO accession GSE113090.

All ChIP-seq raw data were aligned to UCSC human reference genome (hg19) using Bowtie2 software (version2.2.9) and only uniquely aligned reads were retained. Samtools (version 1.3.1) was used to sort aligned reads into genomic order for further analysis. For visualization, sorted BAM files were indexed with Samtools (version 1.3.1) and genome coverage tracks (bigwig files) were generated using Deeptools (version 2.3.1) with parameters of --binsize 10, --extendReads 200. Normalization was performed by reads per genome content (RPGC). H3K4me1 peaks, H3K27ac peaks and differentially regulated H3K27ac regions between MesoT, human coronary artery smooth muscle cells (HCASMC) and human umbilical vein endothelial cells (HUVEC) and were detected using MACS2 (version 2.1.1) by calling broad peaks and differential binding events. All reads were extended from 5' to 3' direction to a final length of 200 bp. The enriched H3K4me1 and H3K27ac peaks were defined as the regions with significant enrichment of FDR < 0.01 relative to respective input control reads. Differentially regulated H3K27ac sites were obtained with a cutoff of $\log_{10}$ likelihood ratio between

two samples. The overlapping regions of H3K4me1 and H3K27ac sites and peaks annotation were analyzed by ChIPseek (http://chipseek.cgu.edu.tw/index.py). Potential primed enhancers were defined as sites which have highly enriched H3K27ac signals in HCASMC and HUVEC compared to MesoT and were also marked with H3K4me1 in MesoT. A list of lineage specific genes with primed enhancers regions in MesoT were obtained in R by intersecting HCASMC- and HUVEC-specific genes (identified as fold change > 4, compared to MesoT, from RNA seq analysis) with annotation tables from potential primed enhancers. The H3K4me1 and H3K27ac heat maps were generated with Deeptools (version 2.3.1). The matrix was built on a list of genes having primed enhancer along with their corresponding H3K4me1 peak regions and signal files of MesoT H3K4me1 bigwig file and HCASMC and HUVEC H3K27ac bigwig files with bin size of 50 bp. The signals were restricted to 5kb around the central region of H3K4me1 peaks. The Gene Ontology enrichment analysis was performed on HCASMC- and HUVEC-specific genes with primed enhancers in MesoTs with Panther (http://pantherdb.org). The GEO accession numbers for HCASMC and HUVEC H3K27ac ChIP-seq are GSM1876036 and GSM1009635, respectively.

Contraction, tube formation, transwell barrier assays

Day 12 SMCs differentiated from MesoT were labeled with DiO per manufacturer's instructions then replated at 3 x 10^5 cells per cm^2 on Geltrex coated 12 well plates (Corning) for 24 hours. Cells were treated with 100 μM carbachol[10] (Sigma), 50 mM KCl[11] or left untreated (control) and monitored for 30 min using a BioTek Lionheart FX. Surface area change for 20 selected cells was measured with ImageJ. For

tube formation assays, MesoT cells were cultured on Matrigel in CDM (-Activin A) supplemented with 50 ng/ml rhVEGF-A_{165} at a density of 1.5 x 10^5 cells/cm^2. Media was changed every other day. Tubes were fixed and probed with antibodies as above.

Endothelial barrier assay ThinCert™ Cell Culture Inserts (pore size 0.4 μm, Greiner Bio-One International) were coated with collagen IV and fibronectin. Cells were seeded onto the PET membrane and cultured at 37°C and 5% CO_2 for 28 days under static conditions in a standard well-plate. Barrier integrity of cells was examined by *trans*-endothelial electrical resistance (TEER) measurements and a FITC-dextran permeability assay. TEER values of the barrier separating the apical and basolateral compartment were determined using a hand-electrode (Millicell ERS-2, Millipore). Permeability of FITC-dextran (40 kDa, Sigma) was measured after application into the apical compartment on an orbital shaker (77 rpm) for 30 min. Cell junctions were visualized by osmium tetroxide contrasting followed by imaging on a JEM-2100 transmission electron microscope (JEOL, Tokyo,Japan).

Transplantation of MesoT cells in a neonatal mechanical injury model

Wt1$^{creERT2/+}$*;Rosa26*$^{tdT/+}$ and *Wt1*$^{+/+}$*;Rosa26*$^{tdT/+}$ neonatal mice were generated by crossing *Wt1*$^{creERT2/+}$ and *Rosa26*$^{tdT/tdT}$ mice and given an intragastric injection of tamoxifen (1 μg, Sigma) dissolved in corn oil on day of birth (D0.5). Six hours after injection, neonatal mice were separated from their mothers and placed on ice for 5 min to induce hypothermia-based anesthesia. Hearts of neonatal mice were mechanically injured as previously described[12]. Briefly, a lateral thoracotomy in the 4th intercostal space was performed to expose the apex of the heart. In the sham operated mice, after the heart was

exposed, the heart was gently placed back into the chest cavity and the rib cage and chest wall were surgically sewn up using 6-0 non-absorbable Prolene sutures. In mechanically injured mice, the heart was resected using iridectomy scissors. In mice receiving treatment with MesoT, 1 million cells labeled with DiO cell labeling solution were suspended in 2 μl of Ca^{2+} and Mg^{2+}-free PBS and injected into the pericardial cavity before sewing up the rib cage and chest wall. Once surgery was complete, neonatal pups were allowed to recover by rapid warming and then returned to their mother. Hearts from each treatment condition were harvested at various times up to 30 days post-injury. Following removal, collected hearts were washed in PBS, fixed in 4% paraformaldehyde for 2 hours then cryo-protected overnight in 30% sucrose solution (both at 4°C) and embedded in OCT. To assess the human cellular contribution to the injury site, cryo-sections of 10 μm thickness were probed with antibodies for human-specific Golgi (TGN46) or human nuclear antigen and cell lineage markers.

Re-cellularization of vascular scaffolds with MesoTs

Jejunal scaffolds were isolated from Lewis rats as described previously[13]. MesoTs were injected through the arterial and venous cannulas into the vascular tree of a decellularized rat jejenum. Optimization of recellularization was achieved by injecting a bolus of cells on three consecutive days. On day 1, 0.5 - 1 x 10^6 cells in 0.5 ml cell culture medium were injected per cannula with an infusion rate of 4 ml/min. Following a one-hour static incubation, allowing for cellular adherence, the injection and static incubation were repeated. To promote functional maturation of the cellular layer on the vascular bed, the scaffold was connected to a bioreactor system to mimic physiological

blood flow conditions by perfusion culture[13]. Cell injection and static adherence were repeated once per arterial and venous cannula per day with subsequent perfusion culture overnight for three consecutive days. After the third day of injection, media was perfused for up to 28 days in the bioreactor. Temperature and CO_2 were maintained at 37ºC and 5%, respectively, with a pressure of 120/80 mmHg. Primary human microvascular endothelial cells (1º ECs) cultured with VascuLife Endothelial Medium (Lifeline Cell Technology) served as control and were loaded as per the first day injection for MesoT cells.

Intravital microscopy was performed to validate recellularized scaffold integrity using a Zeiss inverted microscope after perfusion with carbogen-gassed PBS at 37ºC. FITC-dextran retention and vascular integrity was detected using real-time fluorescence as previously described[14]. Metabolically active cells lining the scaffold vasculature were identified by injecting 1mg/ml of MTT (Serva) in cell culture media for 90 min followed by aspiration and scaffold washing. Recellularized scaffolds were prepared for immunofluorescence analysis by fixation in 4% paraformaldehyde at RT for 2 hours then embedded in paraffin. Deparaffinized sections (5 uM) were dehydrated and stained with specific antibodies. All primary antibodies were incubated over night at 4°C followed by conjugated secondary antibodies for 1 hour at RT. Fluorescence was visualized on a Keyence BZ-9000 fluorescence microscope. For light sheet microscopy (LSM) of cellularized scaffolds, tissue was fixed and then stained with primary antibodies for CD31 and NG2 at 4°C overnight. Conjugated secondary antibodies were then incubated at room temperature for 1 hour followed by optical clearing as previously described[15].

Graft Implantation by Anastomosis

Graft implantation into the abdominal region was conducted in female NIH-*Foxn1*^{rnu} rats (age: 8 weeks, obtained from Charles River). Anesthesia was induced via isoflurane with intraoperative analgesia (Carprofen, 5 mg/kg s.c.). After the abdominal cavity was opened by a median laparotomy, the infrarenal aorta abdominalis and the infrahepatic vena cava were isolated from surrounding tissues. Proximal and distal vessels were clamped and side-to-end anastomosis of the scaffold artery to the aorta abdominalis and vein to the vena cava was performed. Following patency examination and perfusion of blood from the host circulatory system, the abdominal cavity was closed occluding the abdominal musculature and skin was sutured. Grafts were harvested after 3 days for further analysis.

Statistics

qRT-PCR samples were done in technical triplicate and error bars calculated in Microsoft Excel. All other assays and statistical measurements were done in GraphPad Prism 7.0b. SMC contraction assay used one-tailed t-test, Holm-Sidak method to determine statistical significance with alpha=0.05. For carbachol vs. control, the t-ratios for 10, 20 and 30 min, respectively, were 5.551, 5.46 and 5.165 with df=38. For KCl vs. control, the t-ratios for 10, 20 and 30 min, respectively, were 7.62, 7.318 and 5.581 with df=38. p-values were all <0.0001. All error bars are standard error of the mean (SEM) with n=20 for all time points and groups. TEER significance was determined by comparison against 1º ECs using two-way analysis of variance (ANOVA). Dunnett's test corrected for multiple comparisons with 95% confidence interval (CI), alpha=0.05, F-

value=9.376, df=2. Error bars are SEM with n=3 for all measurements. For +VEGF +SB d28 sample vs. 1º ECs, p-value=0.0027. FITC diffusion significance was determined via two-way ANOVA with 1º ECs acting as control for measurements. Control (no cells) were graphed only for visualization. Dunnett's test corrected for multiple comparisons with 95% CI, alpha=0.05, F-value=1.605, df=2. No statistical significance was determined. Errors bars are SEM with n=3 for all measurements. For population doublings, simple linear regression analysis showed a coefficient of determination (R^2) = 0.9774. Experiment n=3 done in technical triplicate. Error bars are SEM. Cell cycle analysis for p4 (n=4) and p9 (n=3) were all done in technical triplicate; error bars are SEM. Clonal multipotency analysis was determined by counting positive cells and plotting the average with n=14 done in technical triplicate.

Table 1 List of Primary Antibodies

Antibody	Application	Supplier	Identifier
Islet-1	IF	R&D systems	Cat#AF1837; RRID:AB_2126324
Nkx2.5 (Clone 259416)	IF	R&D Systems	Cat#MAB2444; RRID:AB_2151378
Wilms Tumor Protein (Clone CAN-R9(IHC)-56-2)	IF, IHC	Abcam	Cat#ab89901; RRID:AB_2043201
ZO-1 (Clone 1)	IF	BD Biosciences	Cat#610966; RRID:AB_398279
Smooth Muscle Actin (Clone 1A4)	IF, IHC	Abcam	Cat#ab7817; RRID:AB_262054
Vimentin (Clone EPR3776)	IF, IHC	Abcam	Cat#ab92547; RRID:AB_10562134
TBX18 (Clone 635305)	IF	R&D Systems	Cat#MAB63371; RRID:AB_10892533
CD140b/PDGFRβ Phycoerythrin Conjugated (Clone 28D4)	FC	BD Biosciences	Cat#558821; RRID:AB_397132
VEGF R3/Flt-4 Allophycocyanin Conjugated (Clone 54733)	FC	R&D Systems	Cat#FAB3492A; RRID:AB_357162
FLT4 (Clone C-20)	IF	Santa Cruz Biotechnology	Cat#sc-321; RRID:AB_2105107
NTRKB	FC	Abgent	Cat#AO2140a; RRID:AB_2714009
CD56/PSA-NCAM (Clone 12F8)	FC, IF	BD Biosciences	Cat#556325; RRID:AB_396363
Flk1	IF	Acris Antibodies GmbH	Cat# AP02618PU-S; RRID:AB_1624459
SOX2 (Clone Y-17)	IF	Santa Cruz Biotechnology	Cat#sc-17320; RRID:AB_2286684
CD31 BD Horizon™ BV421 Conjugated (Clone WM59)	FC	BD Biosciences	Cat#564089; RRID:AB_2714010
CD31 (Clone JC70A)	IF, IHC	Dako	Cat#M0823; RRID:AB_2114471
CD31	IHC	Abcam	Cat#ab28364; RRID:AB_726362
CD31 (Clone P2B1)	IHC	Abcam	Cat#ab24590; RRID:AB_448167
NG2	IF, IHC	Abcam	Cat#ab83508; RRID:AB_2087616
DDR2	IF	Santa Cruz Biotechnology	Cat#sc-7555: RRID:AB_639054
NG2/MCSP Phycoerythrin Conjugated (Clone LHM-2)	FC	R&D Systems	Cat#FAB2585P; RRID:AB_2087615
Anti-Histone H3 (mono methyl K4) antibody - ChIP Grade	ChIP	Abcam	Cat#ab8895; RRID:AB_306847
Anti-Histone H3 (acetyl K27) antibody - ChIP Grade	ChIP	Abcam	Cat# ab4729, RRID:AB_2118291
Calponin	IF	Sigma-Aldrich	Cat#C2687; RRID:AB_476840
Anti-smooth muscle Myosin heavy chain 11 antibody (Clone 1G12)	IF	Abcam	Cat#ab683; RRID:AB_2235569
von Willebrand Factor	IF	Dako	Cat#A0082; RRID:AB_2315602
VE-cadherin	FC	Abcam	Cat#ab33168; RRID:AB_870662
CD73 Phycoerythrin Conjugated (Clone AD2)	FC	BD Biosciences	Cat# 550257; RRID:AB_393561
CD44 Allophycocyanin Conjugated (Clone IM7)	FC	eBioscience	Cat# 17-0441-82; RRID:AB_469390
CD105 BV421 Conjugated (Clone 266)	FC	BD Biosciences	Cat# 563920; RRID:AB_2722606
Human TGN46 (Human Golgi)	IHC	AbD Serotec	Cat#AHP500G; RRID:AB_323104
Nuclei (Human Nuclear Antigen) (Clone 235-1)	IHC	Millipore	Cat#MAB1281; RRID:AB_94090

* Key: IF – immunofluorescence, IHC – immunohistochemistry, FC – flow cytometry, ChIP – chromatin immunoprecipitation

Table 2 List of Secondary and Isotype Control Antibodies

Antibody	Application	Supplier	Identifier
Donkey Polyclonal anti-Mouse IgG (H+L) Alexa Fluor 488 Conjugated	IF, IHC	Thermo Fisher	Cat#:A21202; RRID: AB_141607
Donkey Polyclonal anti-Mouse IgG (H+L) Alexa Fluor 488 Conjugated	IF, IHC	Thermo Fisher	Cat#:A21202; RRID:AB_141607
Donkey Polyclonal anti-Rabbit IgG (H+L) Alexa Fluor 488 Conjugated	IF, IHC	Thermo Fisher	Cat#A21206; RRID:AB_141708
Donkey Polyclonal anti-Goat IgG (H+L) Alexa Fluor 555 Conjugated	IF, IHC	Thermo Fisher	Cat#A21432; RRID:AB_141788
Donkey Polyclonal anti-Mouse IgG (H+L) Alexa Fluor 555 Conjugated	IF, IHC	Thermo Fisher	Cat#A31570; RRID:AB_2536180
Donkey Polyclonal anti-Rabbit IgG (H+L) Alexa Fluor 555 Conjugated	IF, IHC	Thermo Fisher	Cat#A31572; RRID:AB_162543
Donkey Polyclonal anti-Sheep IgG (H+L) Alexa Fluor 647 Conjugated	IHC	Thermo Fisher	Cat#A21448; RRID:AB_2535865
Donkey Polyclonal anti-Goat IgG (H+L) Alexa Fluor 647 Conjugated	IF, IHC	Thermo Fisher	Cat#A21447; RRID:AB_141844
Donkey Polyclonal anti-Rabbit IgG (H+L) Alexa Fluor 647 Conjugated	IF, IHC	Thermo Fisher	Cat#A31573; RRID:AB_2536183
Mouse Monoclonal IgG1 kappa Isotype Control BD Horizon™ BV421 Conjugated (Clone X40)	FC	BD Biosciences	Cat#562438; RRID:AB_11207319
Rat IgG2b kappa Isotype Control Allophycocyanin Conjugated (Clone eB149/10H5)	FC	eBioscience	Cat#17-4031-82; RRID:AB_470176
Mouse Monoclonal IgG1 kappa Isotype Control Phycoerythrin Conjugated (Clone MOPC-21)	FC	BD Biosciences	Cat#555749; RRID:AB_396091
Mouse IgG1 kappa Isotype Control Allophycocyanin Conjugated (Clone P3.6.2.8.1)	FC	eBioscience	Cat# 17-4714-42, RRID:AB_1603315
Mouse IgG1 Isotype Control Allophycocyanin Conjugated (Clone 11711)	FC	R&D Systems	Cat#IC002A; RRID:AB_357239

* Key: IF – immunofluorescence, IHC – immunohistochemistry, FC – flow cytometry

Table 3 Taqman Primers for qRT-PCR

Gene	Supplier	Identifier	Chromosome Location
POU5F1/OCT4	Thermo Fisher	Hs04260367_gH	Chr.6: 31164337 - 31170693
SOX2	Thermo Fisher	Hs01053049_s1	Chr.3: 181711924 - 181714436
NANOG	Thermo Fisher	Hs02387400_g1	Chr.12: 7789396 - 7796061
ISL1	Thermo Fisher	Hs00158126_m1	Chr.5: 51383124 - 51394730
NKX2.5	Thermo Fisher	Hs00231763_m1	Chr.5: 173232104 - 173235312
GATA4	Thermo Fisher	Hs00171403_m1	Chr.8: 11676919 - 11760002
WT1	Thermo Fisher	Hs01103751_m1	Chr.11: 32387775 - 32435535
TBX18	Thermo Fisher	Hs01385457_m1	Chr.6: 84666834 - 84764236
TCF21	Thermo Fisher	Hs00162646_m1	Chr.6: 133889121 - 133895537
RNA18S5	Thermo Fisher	Hs03928985_g1	Chr.Un|NT_167214: 109078 - 110946

References

1. Cliff, T. S. *et al.* MYC Controls Human Pluripotent Stem Cell Fate Decisions through Regulation of Metabolic Flux. *Cell Stem Cell* **21,** 502–516.e9 (2017).
2. Berger, R. P. *et al.* ST8SIA4-Dependent Polysialylation is Part of a Developmental Program Required for Germ Layer Formation from Human Pluripotent Stem Cells. *Stem Cells* **34,** 1742–1752 (2016).
3. Si-Tayeb, K. *et al.* Generation of human induced pluripotent stem cells by simple transient transfection of plasmid DNA encoding reprogramming factors. *BMC Dev. Biol.* **10,** 81 (2010).
4. Wang, L. *et al.* Self-renewal of human embryonic stem cells requires insulin-like growth factor-1 receptor and ERBB2 receptor signaling. *Blood* **110,** 4111–4119 (2007).
5. Takeuchi, M., Takeuchi, K., Ozawa, Y., Kohara, A. & Mizusawa, H. Aneuploidy in immortalized human mesenchymal stem cells with non-random loss of chromosome 13 in culture. *In Vitro Cell. Dev. Biol. Anim.* **45,** 290–299 (2009).
6. Asahina, K. *et al.* Mesenchymal origin of hepatic stellate cells, submesothelial cells, and perivascular mesenchymal cells during mouse liver development. *Hepatology* **49,** 998–1011 (2009).
7. Madisen, L. *et al.* A robust and high-throughput Cre reporting and characterization system for the whole mouse brain. *Nat. Neurosci.* **13,** 133–140 (2010).

8. Zhou, B. & Pu, W. T. Isolation and characterization of embryonic and adult epicardium and epicardium-derived cells. *Methods Mol. Biol.* **843,** 155–168 (2012).

9. Singh, A. M. *et al.* Cell-Cycle Control of Bivalent Epigenetic Domains Regulates the Exit from Pluripotency. *Stem Cell Rep.* **5,** 323–336 (2015).

10. Iyer, D. *et al.* Robust derivation of epicardium and its differentiated smooth muscle cell progeny from human pluripotent stem cells. *Development* **142,** 1528–1541 (2015).

11. Motherwell, J. M. *et al.* Evaluation of Arteriolar Smooth Muscle Cell Function in an Ex Vivo Microvascular Network Model. *Sci. Rep.* **7,** 389 (2017).

12. Porrello, E. R. *et al.* Transient regenerative potential of the neonatal mouse heart. *Science* **331,** 1078–1080 (2011).

13. Kress, S. *et al.* Evaluation of a Miniaturized Biologically Vascularized Scaffold in vitro and in vivo. *Sci. Rep.* **8,** 4719 (2018).

14. Schick, M. A. *et al.* Phosphodiesterase-4 inhibition as a therapeutic approach to treat capillary leakage in systemic inflammation. *J. Physiol. (Lond.)* **590,** 2693–2708 (2012).

15. Brede, C. *et al.* Mapping immune processes in intact tissues at cellular resolution. *J. Clin. Invest.* **122,** 4439–4446 (2012).

CHAPTER 5

FINAL DISCUSSION AND CONCLUSIONS

Mesothelium covers the coelomic organs and functions in development and repair by giving rise to a population of migratory mesothelial cells that invade underlying tissues and differentiate into multiple cell types. This migratory form of mesothelium can act as a vascular progenitor to contribute endothelium, smooth muscle cells and pericytes during *neo*-vascularization. This ability gives mesothelium potentially broad clinical utility in regenerative medicine and tissue repair. We report a robust and efficient differentiation process using hPSCs to generate an *in vitro* equivalent of migratory mesothelium (MesoT) that can be found in various coelomic organs during organogenesis and after injury.

Molecular and transcriptional analysis of hPSC-derived MesoT cells show they are of the mesothelium lineage, express canonical markers such as WT1, TBX18, ALDH1A2 and transition through an epithelial stage consistent with *in vivo* development. Epigenetic analysis of MesoT cells revealed H3K4me1 marks at vascular specific enhancers which places MesoT cells in a primed state and receptive to endothelium and smooth muscle differentiation cues. Their vascular potential was confirmed upon addition of VEGF+SB431542 and PDGFβ to culture media. MesoT-derived endothelium and smooth muscle exhibited functional characteristics such as acetylated-LDL uptake and response to the acetylcholine receptor agonist carbachol and membrane depolarization

agent KCl, respectively. Clonal analysis of MesoT showed the ability to retain multipotency. When used as a cellular therapeutic in a mouse cardiac injury setting, MesoT cells routinely contributed to *neo*-vascularization which is important for tissue repair and possible functional recovery. MesoT cells also displayed utility in tissue engineering by successfully reseeding vascular networks of a decellularized construct. These constructs withstood physiological pressures when connected to the circulatory system of Lewis rats and were able to perfuse blood without experiencing thrombosis or failure after 3 days. While these results were encouraging, testing prolonged durations is warranted.

We argue here that MesoT cells are a migratory form of mesothelium and has potentially broad clinical utility in regenerative medicine by acting as a multipotent vascular progenitor. MesoT cells can generate all the required vascular lineages such as endothelium, smooth muscle and pericytes and self-assemble into vessel-likes structure *in vitro*. The combination of these abilities makes MesoT cells an attractive hPSC-derived source for tissue engineering to create synthetic vessels or add a vascular component in organ reconstruction and building.